

# On the potential of permutation-based repetition coding-like symbol level coding

---

LINUS LARSSON  
MASTER'S THESIS  
DEPARTMENT OF ELECTRICAL AND INFORMATION TECHNOLOGY  
FACULTY OF ENGINEERING | LTH | LUND UNIVERSITY



On the potential of permutation-based  
repetition coding-like symbol level  
coding

Linus Larsson  
li66441a-s@student.lu.se

Department of Electrical and Information Technology  
Lund University

Supervisor: Johan Thunberg, EIT, LTH

Co-supervisor: Juan Vidal Alegría, EIT, LTH

Examiner: Michael Lentmaier, EIT, LTH

June 16, 2025



---

# Abstract

---

The purpose of this thesis is to investigate the potential of transmitting data symbols alongside permuted copies in a repetition coding-like scheme, called the permutation scheme. First exhaustive search is conducted for small constellation sizes to identify possible patterns. The next step was identifying local search methods for permutations, and other methods for longer chains of permutations.

It was found that as permutations are used, the energy efficiency  $d_{min}^2$  of the high-dimensional constellation improves as more and more permutations are used. It was also found that the union bound of a high-dimensional constellation is still indicative of the constellations respective bit error rate performance. Bit error rate was evaluated for the Gaussian channel.

Another seminal investigation was if, and how the permutation scheme could be used alongside binary coding schemes such as block codes. The results show that the block codes do work in conjunction with the permutation scheme, and that random interleaving still functions as expected.

Another property of permutations examined is how optimal permutations for 8-PSK constellations are affected when the constellation points are normalized with respect to different p-norms. We show that energy efficiency (as well as spectral efficiency) is invariant with respect to norm, and a by only using one permutation the scheme outperforms binary signaling with respect to both these metrics.

In terms of future work, a more thorough study is suggested on other methods for finding optimal or near-optimal permutations, including relaxations of optimization problems and heuristics. Furthermore, additional verification of the scheme under different channel models, for example, would be an interesting line of research to pursue. **Keywords:** Channel coding, repetition coding, symbol level coding, permutations, energy efficiency, spectral efficiency



---

## Acknowledgements

---

First, I would like to express my deepest appreciation to my supervisor, Johan Thunberg, EIT, LTH, for introducing me to this particular topic in the first place. I thank him for his invaluable guidance, expertise, and for all the time and effort he committed to this project. I would also like to express my deepest gratitude to my co-supervisor Juan Vidal Alegría, EIT, LTH, for his constructive feedback, helpful advice, and for his resolute encouragement.

I would also like to express my many thanks to my family for all their love and support that I have received during this endeavor. Their encouragement has been my main source of motivation.

Lastly, I'd like to mention the faculty at Lund University for inspiring me, and for setting me on this path.



---

## Popular Science Summary

---

In our modern world it is preferable that wireless communication is as reliable and energy efficient as possible, to which efficient error correcting codes are desirable. In this project, these codes take the form of high-dimensional constellations, and have their symbol alternatives in such locations that the energy efficiency of the transmission can be improved in comparison to underlying uncoded modulation schemes. These symbols are essentially the interface between data bits and physical signals, where the more symbol alternatives a constellation has, the more bits can be packed into a single symbol. In this thesis high-dimensional constellations are investigated, alongside their corresponding symbol error probability bounds and theoretical bit error rates.

These high-dimensional symbol constellations are constructed from an underlying or regular constellation. We refer to the high-dimensional constellation as the counterpart of the regular constellation. When the symbol alternatives in the counterpart are permuted just right, the distance between the symbol alternatives becomes large, meaning that it becomes easier to separate them or detect them, when the physical signal is affected by random noise in a wireless channel.

To actually find these good permutations or the optimal one in the first place, exhaustive search is first conducted for the pulse amplitude modulating scheme (PAM) and the phase shift keying modulating scheme (PSK) in order to identify any and all possible patterns. For constellations with a "too large" number of symbol alternatives, e.g. sixteen, then there are simply too many possible permutations to go through them all. For such cases, when the number of permutations was too large for exhaustive search, we used a greedy local search strategy using randomly selected subsets of permutations.

It was found that such a strategy can be used to improve the energy efficiency of constellations. Like expected, simulations verify that the theoretic increase of energy efficiency resulted in lower bit error rate. In the simulations, the channel was modeled as a signal sent plus additive wide sense stationary Gaussian noise.

The simulations show that the introduced permutation scheme is seemingly compatible with previously established error correcting codes.



---

## List of Acronyms

---

<b>AWGN</b>	Additive White Gaussian Noise
<b>BER</b>	Bit Error Ratio
<b>BPS</b>	bits per second
<b>BPSK</b>	Binary Phase Shift Keying
<b>CS</b>	Constellation Shaping
<b>EE</b>	Energy Efficiency
<b>FSK</b>	Frequency Shift Keying
<b>ML</b>	Maximum-Likelihood
<b>PAM</b>	Pulse Amplitude Modulation
<b>PSD</b>	Power Spectral Density
<b>PSK</b>	Phase Shift Keying
<b>QAM</b>	Quadrature Amplitude Modulation
<b>SNR</b>	Signal-to-Noise Ratio
<b>WSSUS</b>	Wide-Sense Stationary Uncorrelated Scattering
<b>XOR</b>	Exclusive OR operation



---

# Table of Contents

---

<b>1</b>	<b>Introduction</b>	<b>1</b>
1.1	Background . . . . .	1
1.2	Motivation . . . . .	2
1.3	Project aims . . . . .	3
1.4	Limitations . . . . .	3
1.5	Thesis structure . . . . .	4
<b>2</b>	<b>Background</b>	<b>5</b>
2.1	Modulation schemes and channel models . . . . .	5
2.2	Constellation types M-PAM, M-PSK and M-QAM . . . . .	6
2.2.1	M-PAM constellations	6
2.2.2	M-PSK constellations	7
2.2.3	M-QAM constellations	8
2.3	Channel coding . . . . .	10
2.4	Shaping gain and coding gain . . . . .	11
2.5	Permutations . . . . .	11
2.6	Symbol level coding . . . . .	12
2.6.1	Euclidean distance for high-dimensional constellations	12
2.6.2	Energy efficiency for high-dimensional constellations	13
2.7	Theoretical symbol error probability . . . . .	14
2.8	Permutation scheme example . . . . .	14
<b>3</b>	<b>Method and analysis</b>	<b>17</b>
3.1	Exhaustive search of permutations . . . . .	17
3.2	Randomized search of permutations for M-ary constellations . . . . .	19
3.3	8-PSK p-norm normalization . . . . .	20
3.4	Multiple layers of permutation . . . . .	20
3.5	Multiple layers of encoding . . . . .	23
3.6	Overview of collected data for M-PAM, M-PSK and M-QAM permutations . . . . .	24
3.7	Trend analysis and implications for using multiple layers of permutation	24
3.7.1	Distribution of minimum distances for 16-PAM and 16-QAM	24
3.7.2	Union bounds for 16-PAM and 16-QAM	28
3.7.3	Distribution of all distances for 256-QAM constellations	28

3.7.4	256-QAM union bounds	28
3.8	Wireless channel simulation . . . . .	31
3.9	Energy Efficiency and Spectral Efficiency Comparison . . . . .	34
<b>4</b>	<b>Conclusions</b> _____	<b>39</b>
4.1	Summary and conclusions . . . . .	39
4.2	Future work . . . . .	40
	<b>References</b> _____	<b>41</b>
<b>A</b>	<b>Optimal permutations</b> _____	<b>43</b>
<b>B</b>	<b>8-PSK P-norm explanation</b> _____	<b>45</b>

---

## List of Figures

---

2.1	An 8-ary Pulse Amplitude Modulation (PAM) constellation, all adjacent constellation points are equidistant and are centered around the origin point. . . . .	7
2.2	An 8-ary Phase Shift Keying (PSK) constellation, all adjacent constellation points are equidistant and are centered around the origin point. . . . .	8
2.3	An 16-ary Quadrature Amplitude Modulation (QAM) constellation, all adjacent constellation points are equidistant and are centered around the origin point. . . . .	9
3.1	The Energy Efficiency (EE) $d_{min}^2$ versus the value of p that is used for the p-norm for various M-PSK constellations. Only one layer of permutation is used. . . . .	21
3.2	Histogram for the minimum distances in a 16-PAM constellation where one (1) permutation is used. . . . .	27
3.3	Histogram for the minimum distances in a 16-QAM constellation where one (1) permutation is used. . . . .	28
3.4	Plot of the union bound for 16-PAM, where one (1) permutation is used. Regular 4-PAM and uncoded binary signaling (Binary Phase Shift Keying (BPSK)) are used for comparison. . . . .	29
3.5	Plot of the union bound for 16-QAM, where one (1) permutation is used. Regular 4-QAM and uncoded binary signaling (BPSK) are used for comparison. . . . .	29
3.6	Distribution of all distances in a 256-QAM constellation where one (1) permutation is used. . . . .	30
3.7	Distribution of all distances in a 256-QAM constellation where three (3) permutations are used. . . . .	30
3.8	Distribution of all distances in a 256-QAM constellation where five (5) permutations are used. . . . .	31
3.9	Union bound, or the upper symbol error probability bound for 256-QAM where one (1) permutation is used. Regular 16-QAM and uncoded binary signaling (BPSK) are used for comparison. . . . .	32

3.10	Union bound, or the upper symbol error probability bound for 256-QAM where three (3) permutations are used. Regular 16-QAM and uncoded binary signaling (BPSK) are used for comparison. . . . .	32
3.11	Union bound, or the upper symbol error probability bound for 256-QAM where five (5) permutations are used. Regular 16-QAM and uncoded binary signaling (BPSK) are used for comparison. . . . .	33
3.12	Plot of the Bit Error Ratio (BER) for 8-PSK where one (1) permutation is used. Regular 8-PSK and uncoded binary signaling (BPSK) is used for comparison. The number of transmitted information bits is 1 000 000. . . . .	34
3.13	Plot of the BER for 8-PSK where three (3) permutations are used. Regular 8-PSK and uncoded binary signaling (BPSK) is used for comparison. The number of transmitted information bits is 1 000 000. . . . .	35
3.14	Plot of the bit error ratio for 256-QAM where one (1) permutation is used. Regular 16-QAM and uncoded binary signaling (BPSK) is used for comparison. The number of transmitted information bits is 1 000 000. . . . .	35
3.15	Plot of the BER for 256-QAM where three (3) permutations are used. Regular 16-QAM and uncoded binary signaling (BPSK) is used for comparison. The number of transmitted information bits is 1 000 000. . . . .	36
3.16	Plot of the BER for 256-QAM where five (5) permutations is used. Regular 16-QAM and uncoded binary signaling (BPSK) keying is used for comparison. The number of transmitted information bits is 1 000 000. . . . .	36
3.17	Plot of the ideal spectral efficiency compared to the EE of uncoded 256-QAM, the spectral efficiency is calculated for the effective bit rate. Uncoded BPSK is used for comparison. . . . .	37
3.18	Plot of ideal spectral efficiencies vs. the minimum values of $E_b/N_0$ needed to achieve the symbol error probability $P_s = 10^{-5}$ , for various constellations. See tables 3.7, 3.8 and 3.9 for the corresponding number of permutations. The capacity curve is given by $C/W$ , which is derived from Shannon's theorem on channel capacity. . . . .	38

---

## List of Tables

---

3.1	Optimal permutations for an 8-PAM constellation, in terms of the indices for the original constellation points. Only one layer of permutation is used. . . . .	19
3.2	Optimal permutations for an 8-PSK constellation, in terms of the indices for the original constellation points. Only one layer of permutation is used. . . . .	19
3.3	Structure of a high-dimensional constellation when using multiple repetitions with permutations, up to three (3) permutations. $P_0$ represents the constellation points of the original constellation, whereas $P_1, P_2, P_3$ represents permutation matrices $P_i, M \times M$ . Each row represents a permutation of the original constellation points, and each column represents the symbols that has to be sent for a symbol alternative $S_i$ . . . . .	22
3.4	The EE values for M-PAM, also includes the cases where the block code Hamming(7,4) is used, labeled as H(7,4). . . . .	25
3.5	The EE values for M-PSK, also includes the cases where the block code Hamming(7,4) is used, labeled as H(7,4). . . . .	26
3.6	The EE values for M-QAM, also includes the cases where the block code Hamming(7,4) is used, labeled as H(7,4). . . . .	27
3.7	Spectral efficiency $\rho$ and Signal-to-Noise Ratio (SNR) $E_b/N_0$ for $M$ -PAM. The symbol error probability is $P_s = 10^{-5}$ . . . . .	37
3.8	Spectral efficiency $\rho$ and SNR $E_b/N_0$ for $M$ -PSK. The symbol error probability is $P_s = 10^{-5}$ . . . . .	37
3.9	Spectral efficiency $\rho$ and SNR $E_b/N_0$ for $M$ -QAM. The symbol error probability is $P_s = 10^{-5}$ . . . . .	38
A.1	Optimal permutations for a 16-ary PAM constellation, in terms of the indices for the original constellation points. Only one layer of permutation is used. . . . .	43
A.2	Optimal permutation for a 16-ary PSK constellation, in terms of the indices for the original constellation points. Only one layer of permutation is used. . . . .	43

A.3 Optimal permutation for a 16-ary QAM constellation, in terms of the indices for the original constellation points. Only one layer of permutation is used. . . . . 43

## Introduction

## 1.1 Background

In modern times, wireless communication has proven to be an effective method for sending information between mobile devices. However, to achieve this certain requirements should be met such as minimum data rate, coverage, and reliability, etc. .

The data rate measures how much information can be transmitted per second and a precise such metric of the bit rate, which measures the amount of transmitted bits per second (BPS). A bit is the smallest unit of information that can be transmitted. The coverage refers to which areas data can be transmitted from and to.

At the physical layer, for digital communications sequences of  $k$  bits may be represented by  $M = 2^k$  symbols or messages. Each such symbol or message  $m[i]$ , where  $i \in \{1, 2, \dots, M\}$ , is uniquely mapped to a (continuous) signal alternative  $s_i(t) \in \mathcal{S}_{sa} = \{s_l(t)\}_{l=1}^M$ , where  $s_l(t)$  has in general the interval  $[0, T]$  as support for all  $l$ , although not always. Each signal alternative  $s_i(t)$  in  $\mathcal{S}_{sa}$  can, via use of orthonormal basis functions, be represented by a point  $\mathbf{s}_i \in \mathcal{S}_{ss} = \{\mathbf{s}_l\}_{l=1}^M$  in a Euclidean space called the signal space. A modulation scheme or signal constellation is a specific choice of  $\mathcal{S}_{sa}$  or  $\mathcal{S}_{ss}$ , where the visualization of the latter is formally a signal constellation in signal space or a signal space diagram.

In this thesis the potential for coding gain is investigated, when permuted repetitions of signal constellations are used. In this context a permutation  $\sigma$  is a bijection from  $1, 2, \dots, M = \mathbb{N}_M$  to itself (a reordering of the  $M$  integers). A permutation of the signal constellation with  $\sigma$  means that instead of the mapping  $m[i] \rightarrow \mathbf{s}_i$  (or  $m[i] \rightarrow s_i(t)$ ) we use the mapping  $m[i] \rightarrow \mathbf{s}_{\sigma(i)}$  (or  $m[i] \rightarrow s_{\sigma(i)}(t)$ ). Permutations are special cases of rotations, and preserve relative distances and energies of signal alternatives (or equivalently the  $\mathbf{s}_l$ -points in signal space). Also, if a uniform prior probability distribution is assumed (all messages or symbols are equally likely) the average energy per information bit  $E_b$  is invariant under permutations, i.e,

$$E_b = \frac{1}{k} \sum_{l=1}^M E_l = \frac{1}{k} \sum_{l=1}^M E_{\sigma(l)}$$

where  $E_l = |\mathbf{s}_l|_2^2$  for all  $l$ . This, in turns means that for uniform prior, the energy efficiency, defined as

$$d_{\min}^2 = \frac{D_{\min}^2}{2E_b}$$

is invariant under permutations, where  $D_{\min} = \min_{i,j} D_{i,j}$ , where  $D_{i,j} = |\mathbf{s}_i - \mathbf{s}_j|_2^2$ .

Some of the more common modulation schemes include PAM, PSK and QAM. For QAM, both the amplitude and the phase of the signal are modulated. The number in front of a scheme denotes the constellation size, or the number of symbol alternatives in that constellation. The size of the constellation is usually called  $M$ . For example, 16-QAM denotes  $M = 16$ , and there are sixteen symbols or equivalent signal alternatives in that particular modulation scheme.

In the field of channel coding one of the main focuses is to increase the energy efficiency of transmissions.

## 1.2 Motivation

This study is motivated by a search for new strategies of improving reliability in wireless digital communication. To improve the reliability, channel coding such as polar codes and random interleaving is used to increase the performance. The main motivation for this study is to find a symbol level coding scheme that can work in conjunction with existing (binary) coding schemes on the one hand and existing modulation/constellation schemes on the other. By using permutations of symbols, energy efficiency is not changed (for uniform priors) and the envisioned scheme would have the potential to be used on top of existing schemes.

As a motivation for this study, some preliminary experiments have been conducted by the main supervisor with claims that a repetition coding-like permutation-based scheme for 8-PSK with one extra transmission of permuted symbols achieves a higher energy efficiency as well as higher spectral efficiency than binary signaling (that is, 2-PAM or 2-PSK). This is relevant since under repetition coding, binary signaling has the best energy efficiency for classic uncoded modulation schemes, and the energy efficiency declines in general when the constellation size  $M$  is increased, at least for  $M$ -PAM,  $M$ -PSK and  $M$ -QAM.

## 1.3 Project aims

Formally the main goal of this master's thesis is to investigate previously unexplored computationally efficient permutation-based repetition coding-like symbol level coding schemes for potential improvement of energy efficiency and BER. This can be achieved by improving or maximizing the parameter  $d_{min}^2$  over sets of permutation matrices. The aims are as follows:

1. When only one permutation is used, which reduces the bit-rate by 50%, formally prove by means of exhaustive search, what is the energy efficiency for the optimal permutations in terms of maximizing minimum distance in the constellation of symbol pairs for  $M$ -PSK,  $M$ -PAM and possibly  $M$ -QAM for  $M$  is sufficiently small to allow for exhaustive search.
2. Identify patterns appearing for optimal permutations, which provide insight on how the optimal permutations behave for symbol constellations in which the number of symbols  $M$  is too large to allow for exhaustive search.
3. Identify local search methods for finding suboptimal permutations for constellations where the number of symbols  $M$  is too large for exhaustive search of permutations, and identify bounds for optimal permutations.
4. When one permutation is used, investigate how optimal permutations for 8-PSK are affected when normalizing each constellation point  $\mathbf{z}_l$  with the value of the p-norm applied to itself, namely  $\mathbf{z}_l \rightarrow \frac{\mathbf{z}_l}{\|\mathbf{z}_l\|_p}$ .  $\mathbf{z}_l$  represents a complex valued, high-dimensional constellation point on the form  $\mathbf{z}_l = [z_{l,1}, z_{l,2}, \dots, z_{l,n/2}]$ , where each element represents a point in a 2D-constellation.
5. Investigate how more permutations than one can be used for more channel uses with the aim to further improve energy efficiency.
6. Identify how the proposed permutation schemes can be used in conjunction with binary coding schemes to improve energy efficiency beyond what is attained when binary coding schemes are used with some naive/uncoded modulation scheme such as binary antipodal signaling.

## 1.4 Limitations

This study will only focus on the three  $M$ -ary constellations  $M$ -PAM,  $M$ -PSK and  $M$ -QAM while all other modulation schemes are disregarded. The project is based on theoretical analysis, which includes a simplistic simulation whose wireless channel only considers complex Additive White Gaussian Noise (AWGN) while disregarding any and all other factors. The only binary coding schemes that are used in the simulation is the block code Hamming(7,4). Not all of the optimal permutations can be found with the described methods, so some results may be suboptimal.

## 1.5 Thesis structure

The report is structured as follows: The background section gives necessary information to understand the results, and is succeeded by the method and analysis section, which follows the structure outlined in the project aims section. The analysis is in turn followed by a results section where the major results are outlined, and discussed. The final part of the main report consists of the conclusions drawn from the discussion. Finally there is a set of appendices that contains all relevant results that did not fit in the main report.

## 2.1 Modulation schemes and channel models

As mentioned in the introduction, data can be represented by bits, which in turn can be represented by symbols. These symbols are a compact form of representing sequences of  $k$  bits, and thus can increase the overall data transfer rate. As the bits are mapped to symbols, the symbols in turn affect the baseband transmitted physical signal  $s(t) = g(t)A \sin(2\pi ft + \phi)$ , where  $g(t)$  is the pulse shape,  $A$  is the amplitude,  $f$  is the frequency and  $\phi$  is the phase of the signal respectively [10]. By modulating the amplitude, frequency or the phase of the signal, a receiver will then be able to tell the different waveforms apart, and will thus be able to identify the transmitted symbols.

The different ways of modulating a signal are organized into modulation schemes, and some of the more common ones are PAM, Frequency Shift Keying (FSK), PSK and QAM. Depending on the structure of the modulation scheme they have various EE, and thus various resilience against random noise in a wireless channel for the same SNR. Out of the previously mentioned modulation schemes, the advantage with QAM is that two separate signal components are transmitted simultaneously, namely the inphase and the quadrature component. This way, QAM can be seen as transmitting two separate PAM signals at the same time.

For wireless channels, the most common assumption is the so-called Wide-Sense Stationary Uncorrelated Scattering (WSSUS) assumption, meaning that the statistical properties of a channel do not change over time, and that all received signal contributions with different delays are uncorrelated [11]. Commonly included factors for channel modeling is the free-space path loss, affected by distance, the large-scale fading which occurs when an object is larger or much larger than the wavelength of the signal, and small-scale fading which occurs when several received signal components interfere at the receiver, usually caused by multi-path propagation [11].

Another important factor for channel modeling is random noise, which directly affects the transmitted signal. For several models it is assumed that the noise is additive, has a mean of zero, and has the same Power Spectral Density (PSD) for

all frequencies, so-called AWGN [10]. In some other cases, the PSD of the noise may not be constant, resulting in so-called colored noise. For any type of noise, the noise may cause the received symbols to go beyond the decision boundary of a constellation point, resulting in an incorrectly decoded symbol.

## 2.2 Constellation types M-PAM, M-PSK and M-QAM

For the following types of constellations, the constellation points are in this report represented using complex numbers on the form  $z = a + ib, z \in \mathbb{C}$ . In polar form the points can be written like  $z = Ae^{iv}$ , where  $A$  is the amplitude, and  $v$  is the phase, or angle.

### 2.2.1 M-PAM constellations

For  $M$ -PAM the signal alternatives  $s_l(t)$  may be expressed as (2.1), [10, Eq. (2.38)] where  $A_l$  is the modulating amplitude,  $g(t)$  is the base pulse and  $T_s$  is the symbol duration. The amplitudes  $A_l$  may be represented by equation (2.2), [10, Eq. (2.39)], and an example for 8-PAM is shown in figure 2.1.

$$s_l(t) = A_l g(t), 0 \leq t \leq T_s, l = 0, 1, \dots, M - 1 \quad (2.1)$$

$$A_l = -M + 1 + 2l, l = 0, 1, \dots, M - 1 \quad (2.2)$$

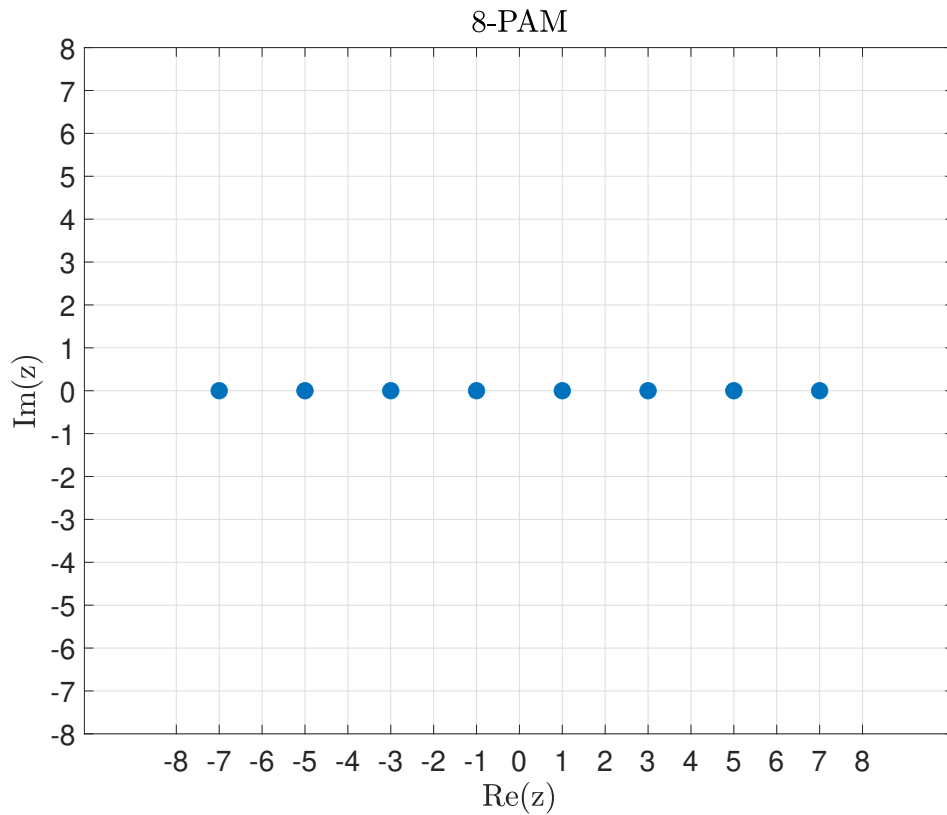


**Figure 2.1:** An 8-ary PAM constellation, all adjacent constellation points are equidistant and are centered around the origin point.

## 2.2.2 M-PSK constellations

For  $M$ -PSK the signal alternatives  $s_l(t)$  may be expressed as (2.3), [10, Eq. (2.54)] where  $g(t)$  is the base pulse,  $f_c$  is the carrier frequency,  $v_l$  is the modulating phase and  $T_s$  is the symbol duration. The phases  $v_l$  may be represented by equation (2.4), [10, Eq. (2.57)], and an example for 8-PSK is shown in figure 2.2.

$$s_l(t) = g(t) \cos(2\pi f_c t + v_l), \quad 0 \leq t \leq T_s, \quad l = 0, 1, \dots, M - 1 \quad (2.3)$$

$$v_l = 2\pi l/M + v_{const}, \quad v_{const} = 0, \quad l = 0, 1, \dots, M - 1 \quad (2.4)$$

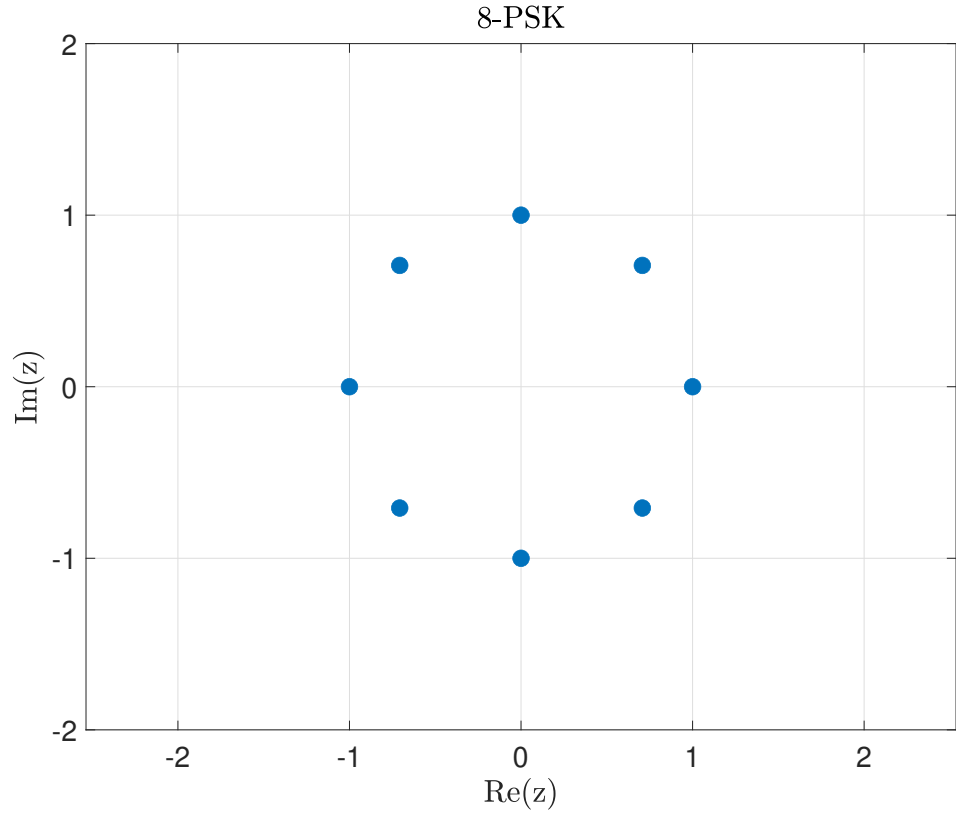


**Figure 2.2:** An 8-ary PSK constellation, all adjacent constellation points are equidistant and are centered around the origin point.

### 2.2.3 M-QAM constellations

For  $M$ -QAM the signal alternatives  $s_l(t)$  may be represented as (2.5), [10, Eq. (2.87)] where  $A_l$ ,  $B_l$  are the amplitudes for the inphase- and quadrature components respectively,  $g(t)$  is the base pulse,  $f_c$  is the carrier frequency and  $T_s$  is the symbol duration. The amplitudes  $A_l$ ,  $B_l$  may be represented by equation (2.6), [10, Eq. (2.96), Eq. (2.97)] and an example for 16-QAM can be seen in figure 2.3.

$$s_l(t) = A_l g(t) \cos(2\pi f_c t) - B_l g(t) \sin(2\pi f_c t), \quad 0 \leq t \leq T_s, \quad l = 0, 1, \dots, M-1 \quad (2.5)$$

$$\begin{aligned} & \{(A_l, B_l)\}_{l=0}^{M-1} \\ & A_l \in \{-\sqrt{M} + 1 + 2i\}_{i=0}^{\sqrt{M}-1} \\ & B_l \in \{-\sqrt{M} + 1 + 2i\}_{i=0}^{\sqrt{M}-1} \end{aligned} \quad (2.6)$$

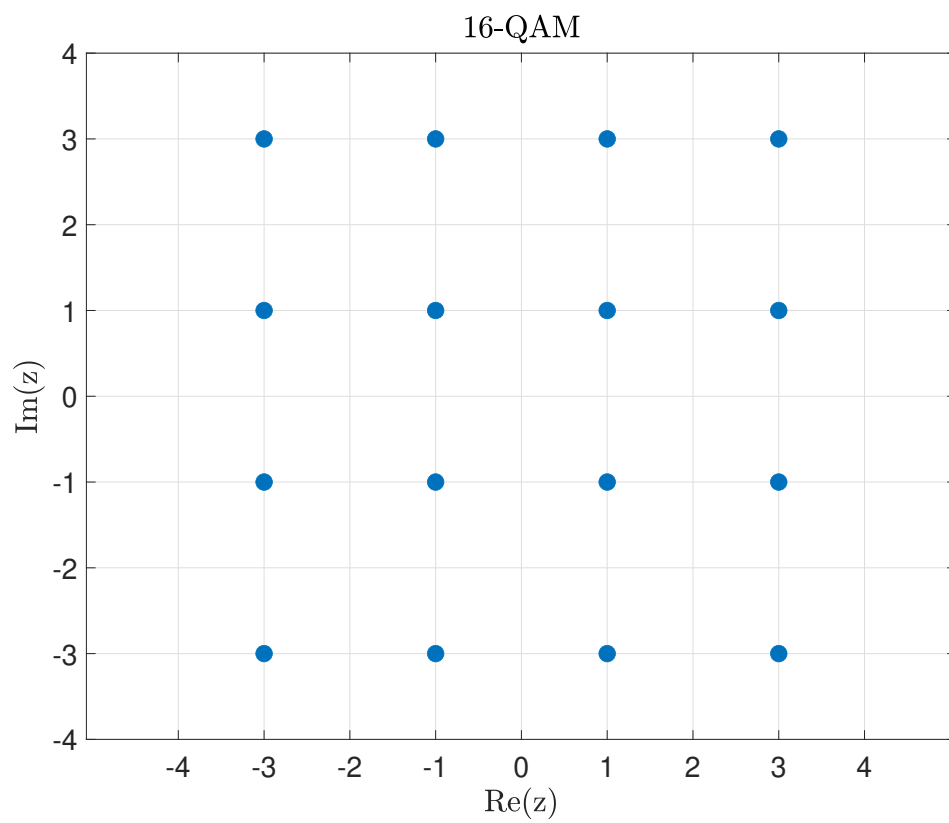


**Figure 2.3:** An 16-ary QAM constellation, all adjacent constellation points are equidistant and are centered around the origin point.

## 2.3 Channel coding

The purpose of channel coding is primarily to add redundant information to data in such a way that incorrectly received bits can be detected, or even corrected by various coding techniques. The field of channel coding has its roots in the works presented by C.E. Shannon, one of them being the capacity theorem  $C = W \log_2 \left(1 + \frac{P}{N}\right)$ , which asserts that there is a maximum rate for data transfer,  $R < C$  [13]. The theorem states that reliable communication is only possible if the bit rate is equal to or less than the capacity  $C$ , at which point the error can be made to be arbitrarily small [13].  $W$  represents the bandwidth, and  $P/N$  the SNR.

Ideally, capacity can be reached while using a fixed value of SNR. To accomplish this goal, error correcting codes are created and used in transmissions. One of the earlier error correcting codes is the Hamming code designed by R.W Hamming, which adds redundant parity bits in such a way that the status of each bit is monitored by at least one parity bit, allowing the code to correct at least single bit errors [8]. In the case of the code Hamming(7,4), three parity bits are added to sequences of four bits, enabling single-bit correction, and double-bit detection (but not correction).

Later on the Hamming codes would serve as inspiration for the more general block codes devised by P. Elias, [6]. As in the case with Hamming codes, the general strategy is to divide the bits into messages, which can then be encoded into codewords, or blocks. These codewords can then ideally be decoded at the receiver, and have all the original information extracted from them. At a later point, A. Viterbi would show that the class of codes known as convolutional codes have the potential to be better than block codes for the same code length, [14]. When convolutional codes are used the bits are not encoded into blocks, instead logical operations are performed upon a continuous stream of bits, where the value of an encoded bit is affected by a certain number of succeeding bits. A notable example of a decoder is the Viterbi algorithm, in which the receiver will iterate over sequences of bits and determine which bits (the options are always the bit "1" or "0") are more likely to be correct [14]. It is not practical for the receiver to consider all received bits at the same time, since the number of possible options grows exponentially  $n_{options} = 2^{n_{bits}}$  with the number of received bits.

The error correcting turbo-codes were devised by C. Berrou, A. Glavieux, and P. Thitimajshima, and are in principle a distinct class of convolutional codes that is near the Shannon capacity limit  $C/W$  [4]. The core feature of turbo-codes are the two recursive convolutional encoders that work in parallel, and a recursive feedback decoder. It is shown in the paper [4] that as the number of iterations in the recursive feedback decoder increases, the binary error rate sharply declines for the same SNR.

The Low-Density Parity-Check (LDPC) codes were created by R. G. Gallager, and are characterized by a parity-check matrix that has a large number of zeros, and a small number of ones, hence low-density [7]. These parity-check matrices

are constructed from information and check digits, and while it is not optimal in the sense of minimizing error probability, the author asserts that there is a non-complex decoding scheme for these low-density codes as compensation. The check digits can be generated by using binary addition on sets of information digits, which is equivalent to using the logical operation Exclusive OR operation (XOR).

The polar code method was developed by E. Arikan, and primarily combines and divides identical binary channels into reliable- and unreliable channels, where information bits are only sent through the reliable ones [2]. For the unreliable channels the bits are usually set to all zeros, which is referred to as frozen bits. The input bits are encoded using a generator matrix and are decoded using successive cancellation, allowing the polar code to reach Shannon capacity as the block size  $N$  approaches infinity [2].

## 2.4 Shaping gain and coding gain

The primary idea behind shaping gain for QAM constellations is to not let all symbol alternatives be equally likely. Instead the probability distribution for the symbols is altered in such a way that the constellation may be closer to reach capacity, as stated in [9]. To lower the average power, symbols close to the origin point have a higher probability of being chosen compared to symbol alternatives further away. Formally the method is known as Constellation Shaping (CS), and ideally does not affect neither the data rate  $R_b$ , nor the necessary bandwidth  $W$ . Note that the permutation scheme does not make use of CS.

Coding gain refers to the practice of using error-correcting codes in order to lower the minimum SNR needed for a certain symbol error probability, and is defined as the difference in necessary SNR to achieve a certain BER between a coded and an uncoded system. Several examples of error-correcting codes can be found in the previous section. Overall, both classes of aforementioned methods have the aim of decreasing the minimum transmission power, and can with advantage be used at the same time.

## 2.5 Permutations

Permutation refers to the mathematical concept where the order, or the re-ordering of selected (or all) elements from a set is significant. This is unlike the concept of combinations, where the order of elements is not significant. Permutations can typically be denoted with the symbol  $\sigma$ . In the context of this report high-dimensional constellations will be denoted with the prefix "hyper-".

Permutation codes are a class of error-correcting codes that permute the order of bits or symbols, which relies on the receiver already knowing the original order of symbols. A notable example are the turbo-codes where interleaving is used as a step in the overall process [4]. Another way of using permutation is the so-called

gray coding scheme, where two adjacent symbol alternatives will only differ in one bit, reducing the number of bits that is received incorrectly [10].

## 2.6 Symbol level coding

In symbol level coding the data symbols are encoded using a scheme before transmission, in order to decrease BER. Coded modulation refers to schemes that combine coding and modulation in a particular way to improve the spectral efficiency and BER of communication systems. Traditionally, channel coding and modulation were treated as separate blocks in the design of communication systems. However, combining these two techniques can make use their interdependence, leading to theoretically better error performance. A notable aspect is that demodulation on symbol level coding could be complex. However, the permutation scheme could be a compromise between increased complexity and better error performance.

In the case of the permutation-based repetition coding-like coding scheme, there is one or several permuted versions of the original constellation, and as such the data symbols are transmitted alongside the symbols from the permuted constellation(s). For instance, when a single permutation is used every other symbol in the transmission will be a data symbol, while the other half of the transmitted symbols will be redundant permutation symbols. See (2.7) for an example of a permutation matrix with dimensions  $4 \times 4$ , which can then be used to permute a constellation with  $M = 4$  symbol alternatives.

In order to improve the EE for the resulting high-dimensional constellation, the symbols are permuted in such a way that the minimum distance between the symbol alternatives is as large as possible. Assuming that all the relevant n-dimensional signal spaces are Euclidean spaces, the distances in a n-dimensional constellation can be calculated using the Euclidean norm as shown in equation (2.8), where each  $x_i$  is a coordinate for a n-dimensional point.

$$P_{i,4x4} = \begin{pmatrix} 1 & 0 & 0 & 0 \\ 0 & 0 & 0 & 1 \\ 0 & 1 & 0 & 0 \\ 0 & 0 & 1 & 0 \end{pmatrix} \quad (2.7)$$

$$\|x\|_2 := \sqrt{x_1^2 + \dots + x_n^2} \quad (2.8)$$

### 2.6.1 Euclidean distance for high-dimensional constellations

For convenience all constellation points are represented as complex numbers,  $z_i = x_i + iy_i$ ,  $z_i \in \mathbb{C}$ ,  $z_i \neq 0$ , meaning that equation (2.8) can be rewritten to be in terms of real- and imaginary components instead, see equation (2.9) where  $n/2$  is the number of constellation points for a symbol alternative.

$$\|\mathbf{z}_i\|_2 = \sqrt{\text{Re}(z_{i,1})^2 + \text{Im}(z_{i,1})^2 + \cdots + \text{Re}(z_{i,n/2})^2 + \text{Im}(z_{i,n/2})^2} \quad (2.9)$$

Similarly the Euclidean distance between two symbol alternatives  $S_i$  and  $S_j$  can be written as  $D_{i,j} = \|\mathbf{z}_i - \mathbf{z}_j\|_2$

$$= \left( (\text{Re}(z_{i,1}) - \text{Re}(z_{j,1}))^2 + (\text{Im}(z_{i,1}) - \text{Im}(z_{j,1}))^2 + \cdots \right. \\ \left. + (\text{Re}(z_{i,n/2}) - \text{Re}(z_{j,n/2}))^2 + (\text{Im}(z_{i,n/2}) - \text{Im}(z_{j,n/2}))^2 \right)^{1/2} .$$

## 2.6.2 Energy efficiency for high-dimensional constellations

As seen in [10, Eq. (4.117)] the EE can be written as  $d_{min}^2 = \frac{D_{min}^2}{2E_b}$ , where  $D_{min}^2$  is the minimum squared Euclidean distance in the constellation, and  $E_b$  is the average energy per bit. In the case where one permutation is used,  $E_b$  can in turn be written as in equation (2.10) (since both the original and permuted constellation have the same symbol energies, and thus double the energy is needed to transmit a set of bits) as shown in [10, Eq. (4.115)], where the results of [10, Eq. (2.29), Eq. (5.6)] were used. In equation (2.10)  $M$  is the constellation size,  $k$  is the number of bits per symbol,  $k = \log_2(M)$  and  $E_i$  is the symbol energy for symbol alternative  $S_i$ . For complex vectors their absolute values are equivalent to equation (2.9).

$$E_b = \frac{1}{k} \times \frac{1}{M} \times 2 \sum_{i=0}^{M-1} E_i, \quad E_i = |\mathbf{z}_i|^2 \quad (2.10)$$

In the case where at least one error correcting code is use,  $E_b$  is given by equation (2.11), where  $R$  is the total coding rate.

$$E_b = \frac{1}{k} \times \frac{1}{M} \times \frac{1}{R} \times 2 \sum_{i=0}^{M-1} E_i, \quad E_i = |\mathbf{z}_i|^2 \quad (2.11)$$

In the case of uncoded  $M$ -PAM,  $M$ -PSK and  $M$ -QAM, the EE can be simplified to  $d_{min}^2 = \frac{6 \log_2(M)}{M^2-1}$ ,  $d_{min}^2 = 2 \sin^2(\pi/M) \log_2(M)$  and  $d_{min}^2 = \frac{3 \log_2(M)}{M-1}$  respectively, [10, (Table 5.1)].

$$d_{min,PAM}^2 = \frac{6 \log_2(M)}{M^2 - 1} \quad (2.12)$$

$$d_{min,PSK}^2 = 2 \sin^2(\pi/M) \log_2(M) \quad (2.13)$$

$$d_{min,QAM}^2 = \frac{3 \log_2(M)}{M - 1} \quad (2.14)$$

## 2.7 Theoretical symbol error probability

For digital communications, the upper bound for symbol error probability  $P_s$ , or the union bound, is given by equation (2.15), [10, Eq. (4.106)], where  $P_j$  is the probability of message  $m_j$  being sent,  $D_{i,j}^2$  is the squared Euclidean distance between the symbol alternatives  $S_i$  and  $S_j$ ,  $N_0$  is the noise power in watts [w], and the Q-function is in turn given by equation (2.16), [10, Eq. (3.157)].

$$P_s \leq \sum_{j=0}^{M-1} P_j \sum_{\substack{i=0 \\ i \neq j}}^{M-1} Q \left( \sqrt{\frac{D_{i,j}^2}{2N_0}} \right) \quad (2.15)$$

$$Q(x) = \int_x^{\infty} \frac{1}{\sqrt{2\pi}} e^{-y^2/2} dy = 1 - Q(-x) \quad (2.16)$$

When multiple permutations are used, the union bound (2.15) can be rewritten to (2.17), where  $c_i$  is the number of occurrences for the distance  $d_i$  in the high-dimensional constellation. The union bound in this context is the block-wise error probability since the permutation scheme is repetition-coding like, meaning that the decoding decision is made for an entire block of symbols. The values  $c_i$  are found by computing all  $\frac{M(M-1)}{2}$  distances  $D_{i,j}$  in the constellation and then counting the number of occurrences of each distance.

$$P_s \leq \frac{c_1}{M} Q \left( \sqrt{d_1^2 \frac{E_b}{N_0}} \right) + \dots + \frac{c_k}{M} Q \left( \sqrt{d_k^2 \frac{E_b}{N_0}} \right) \quad (2.17)$$

## 2.8 Permutation scheme example

As an example of the permutation scheme being used, consider an 8-PSK constellation where one permutation is used, and where a constellation point has the energy  $E_s = 1$ . Normally for 8-PSK, the minimum squared Euclidean distance is  $D_{min}^2 = 4E_s \sin^2(\pi/M) = 4 \times 1 \times \sin^2(\pi/8) \approx 0.5858$ , and has the average energy per bit  $E_b = E_s / \log_2(M) = 1 / \log_2(8) = 1/3$  [10, Eq. (5.43), Eq. (2.31)]. This gives the constellation an EE of  $d_{min}^2 = \frac{D_{min}^2}{2E_b} = \frac{0.5858}{2 \times 0.3333} \approx 0.879$ .

However, when a permutation is used to construct a high-dimensional constellation, the value of the new minimum Euclidean distance  $D_{min}$  will have contributions from both the original constellation points and the permuted ones. In the case of 8-PSK, assume we have the original constellation points  $\mathbf{z}_{org} = [1, \frac{1}{\sqrt{2}} + i\frac{1}{\sqrt{2}}, i, -\frac{1}{\sqrt{2}} + i\frac{1}{\sqrt{2}}, -1, -\frac{1}{\sqrt{2}} - i\frac{1}{\sqrt{2}}, -i, \frac{1}{\sqrt{2}} - i\frac{1}{\sqrt{2}}]$ , and that we have a permuted version  $\mathbf{z}_{perm} = [1, -\frac{1}{\sqrt{2}} + i\frac{1}{\sqrt{2}}, -i, \frac{1}{\sqrt{2}} + i\frac{1}{\sqrt{2}}, -1, \frac{1}{\sqrt{2}} - i\frac{1}{\sqrt{2}}, i, -\frac{1}{\sqrt{2}} - i\frac{1}{\sqrt{2}}]$ , which all have the energy  $E_s = |\mathbf{z}_{org,1}|^2 = (1-0)^2 + (0-0)^2 = 1$  since it is a  $M$ -PSK constellation. By calculating all  $\frac{M(M-1)}{2} = \frac{8 \times (8-1)}{2} = 28$  distances  $D_{i,j}$ , it can be found that the squared minimum distance  $D_{min}^2$  appears for the high-dimensional constellation point pair  $(\mathbf{z}_1, \mathbf{z}_2) = ([\mathbf{z}_{org,1}, \mathbf{z}_{perm,1}], [\mathbf{z}_{org,2}, \mathbf{z}_{perm,2}]) = ([1, 1], [\frac{1}{\sqrt{2}} + i\frac{1}{\sqrt{2}}, -\frac{1}{\sqrt{2}} + i\frac{1}{\sqrt{2}}])$ . This results in the squared minimum distance

$D_{min}^2 = D_{1,2}^2 = \|\mathbf{z}_1 - \mathbf{z}_2\|_2^2 = (1 - \frac{1}{\sqrt{2}})^2 + (0 - \frac{1}{\sqrt{2}})^2 + (1 - (-\frac{1}{\sqrt{2}}))^2 + (0 - \frac{1}{\sqrt{2}})^2 = \frac{3}{2} - \sqrt{2} + \frac{1}{2} + \frac{3}{2} + \sqrt{2} + \frac{1}{2} = \frac{8}{2} = 4$ . Since two symbols now carry the same information the average energy per information bit  $E_b$  doubles, becoming  $E_b = 2 \times \frac{E_s}{\log_2(M)} = 2 \times \frac{1}{\log_2(8)} = \frac{2}{3}$ . This all results in the increased EE  $d_{min}^2 = \frac{4}{2 \times \frac{2}{3}} = 3$ , meaning that the EE has significantly improved compared to the original constellation. With an increased EE, the resilience of the signals against random noise in wireless channels is expected to improve.



---

Method and analysis

---

### 3.1 Exhaustive search of permutations

Since the number of possible permutations grows in a factorial sense as the constellation size  $M$  increases,  $n_{perm} = M! = M \cdot (M - 1) \cdots 2 \cdot 1$  exhaustive search for optimal permutations is only feasible for small enough values of  $M$ . In the case when  $M$  is a small value, like  $M = 8$  all possible permutations of the indices for the constellation points are generated. For a constellation size  $M$ , there are  $\binom{M}{2} = \frac{M(M-1)}{2}$  unique symbol pairs, and thus  $\frac{M(M-1)}{2}$  unique Euclidean distances in the constellation. To find the optimal permutation(s), the minimum Euclidean distance  $D_{min}$  for each choice of permutation has to be obtained by calculating all  $\frac{M(M-1)}{2}$  distances  $D_{i,j}$  in the resulting high-dimensional constellation, and subsequently choosing  $D_{min} = \min_{i,j} D_{i,j}$ . The optimal permutation is then the one that generates the maximum  $D_{min}$  for a high-dimensional constellation. For convenience, some of the equations from the background chapter are restated below: the Euclidean distance (3.1), and EE (3.2)

$$\begin{aligned}
D_{i,j} &= \|\mathbf{z}_i - \mathbf{z}_j\|_2 \\
&= \left( (\operatorname{Re}(z_{i,1}) - \operatorname{Re}(z_{j,1}))^2 + (\operatorname{Im}(z_{i,1}) - \operatorname{Im}(z_{j,1}))^2 + \cdots \right. \\
&\quad \left. + (\operatorname{Re}(z_{i,n/2}) - \operatorname{Re}(z_{j,n/2}))^2 + (\operatorname{Im}(z_{i,n/2}) - \operatorname{Im}(z_{j,n/2}))^2 \right)^{1/2} \quad (3.1)
\end{aligned}$$

$$d_{min}^2 = \frac{D_{min}^2}{2E_b} \quad (3.2)$$

Exhaustive search is feasible when  $M \leq 9$ . The algorithm for finding the best permutation in a list of permutations can be seen Algorithm 1:

---

**Algorithm 1:** Search for Best Permutations in List

---

**Input:** List of permutations  $\mathcal{L}$ , constellation size  $M$ , constellation points  $\mathbf{z}_1, \mathbf{z}_2, \dots, \mathbf{z}_M$

**Output:** List of best permutations, best  $d_{\min}^2$

- 1 Store each permutation  $\sigma$  from list  $\mathcal{L}$  in matrix  $\mathcal{P}$ ;
- 2 **foreach** permutation  $\sigma \in \mathcal{P}$  **do**
- 3     Permute constellation points using  $\sigma$  and store as  $\mathbf{Z}_\sigma$ ;
- 4     Set  $D_{\min, current}^2 \leftarrow \infty$ ;
- 5     **foreach** pair  $(i, j)$  of distinct points in  $\mathbf{Z}_\sigma$  **do**
- 6         Calculate  $D_{i,j}^2$  using (3.1);
- 7         **if**  $D_{i,j}^2 < D_{\min, current}^2$  **then**
- 8             Set  $D_{\min, current}^2 \leftarrow D_{i,j}^2$ ;
- 9     **if**  $D_{\min, current}^2 = D_{\min, best}^2$  **then**
- 10         Add  $\sigma$  to list of best permutations;
- 11     **else**
- 12         **if**  $D_{\min, current}^2 > D_{\min, best}^2$  **then**
- 13             Clear list of best permutations;
- 14             Add  $\sigma$  to list of best permutations;
- 15             Set  $D_{\min, best}^2 \leftarrow D_{\min, current}^2$ ;
- 16 Calculate and display the EE  $d_{\min, best}^2$  using (3.2);
- 17 Display the list of best permutations;

---

The permutations found via exhaustive search (meaning that all possible permutations  $\sigma$  were generated) for 8-PAM and 8-PSK are stored in the tables 3.1 and 3.2 respectively. When using the permutations in table 3.1 for 8-PAM, the theoretical EE is  $d_{\min}^2 = 1.143$ , with twenty optimal permutations being found. The permutations listed in the table suggests that optimal permutations should have a cyclical structure, and that every optimal permutation has a reverse counterpart. A cyclical structure in this case refers to previously adjacent constellation points now being separated with a certain amount of steps. When using the permutations in table 3.2 for 8-PSK, the theoretical EE is  $d_{\min}^2 = 3.0$ , with sixteen optimal permutations being found. Like in the case of 8-PAM, the resulting permutations in the table are cyclical in nature, and seemingly every optimal permutation has a reverse counterpart. Compared to 8-PAM, there are fewer optimal permutations which can be explained by the added restrictions that 8-PSK constellations has; namely the fact that for M-PSK the first- and last symbol alternatives  $S_i$  are adjacent, unlike for M-PAM.

8-PAM permutations

1 4 7 2 5 8 3 6  
1 6 3 8 5 2 7 4  
2 5 8 3 6 1 4 7  
2 7 4 1 6 3 8 5  
3 6 1 4 7 2 5 8  
3 6 1 8 5 2 7 4  
3 8 5 2 7 4 1 6  
4 1 6 3 8 5 2 7  
4 7 2 5 8 1 6 3  
4 7 2 5 8 3 6 1  
5 2 7 4 1 6 3 8  
5 2 7 4 1 8 3 6  
5 8 3 6 1 4 7 2  
6 1 4 7 2 5 8 3  
6 3 8 1 4 7 2 5  
6 3 8 5 2 7 4 1  
7 2 5 8 3 6 1 4  
7 4 1 6 3 8 5 2  
8 3 6 1 4 7 2 5  
8 5 2 7 4 1 6 3

**Table 3.1:** Optimal permutations for an 8-PAM constellation, in terms of the indices for the original constellation points. Only one layer of permutation is used.

8-PSK permutations

1 4 7 2 5 8 3 6  
1 6 3 8 5 2 7 4  
2 5 8 3 6 1 4 7  
2 7 4 1 6 3 8 5  
3 6 1 4 7 2 5 8  
3 8 5 2 7 4 1 6  
4 1 6 3 8 5 2 7  
4 7 2 5 8 3 6 1  
5 2 7 4 1 6 3 8  
5 8 3 6 1 4 7 2  
6 1 4 7 2 5 8 3  
6 3 8 5 2 7 4 1  
7 2 5 8 3 6 1 4  
7 4 1 6 3 8 5 2  
8 3 6 1 4 7 2 5  
8 5 2 7 4 1 6 3

**Table 3.2:** Optimal permutations for an 8-PSK constellation, in terms of the indices for the original constellation points. Only one layer of permutation is used.

## 3.2 Randomized search of permutations for M-ary constellations

As mentioned above, when the constellation size  $M$  is too large, exhaustive search is no longer feasible. Instead, the permutations are either randomly generated or based on conjectures of what they could be.

Conjecture 1 (from main supervisor): when  $\sqrt{M}$  is an integer, there is a specific cyclic pattern of the permutation matrix that is conjectured to be the minimum-distance maximizing permutation for at least  $M$ -PAM. For that particular  $M$ -PAM conjecture, there are then  $\sqrt{M}$  symbols adjacent to each other in groups, and the difference of the indices between two adjacent elements in a group is then  $\sqrt{M}$ .

Conjecture 2 (author’s conjecture): for  $M$ -PSK constellations, the optimal permutations are cyclical, since the constellation points are placed on a circle and the first and last constellation points are adjacent.

Conjecture 3 (author’s conjecture): for  $M$ -QAM constellations, the optimal permutations can be found by placing constellation points in a cyclical pattern, where there is a fixed number of steps between previously adjacent symbols, and then permuting the rows of the constellation. The points are indexed from the up-leftmost point, going to the right at each row before going down to the next one, finally ending at the down-rightmost point. Using this method, instead of permuting individual constellation points, entire groups of points are permuted instead. It is also conjectured that optimal  $M^2$ -QAM permutations can be found from optimal  $M$ -PAM permutations, which is linked with the previously mentioned conjecture.

The algorithm for finding optimal (or at least acceptable) permutations is the same as in the previous section, with the exception that instead of generating all possible permutations, only a set amount are (randomly) generated.

### 3.3 8-PSK $p$ -norm normalization

For 8-PSK it is conjectured that if the original constellation points  $z_i$  are normalized using their respective  $p$ -norms, see equations (3.3), (3.4) then  $d_{min}^2 = 3, p \geq 2$  after the constellation points have been permuted. A possible explanation for the conjecture can be found in appendix B.

$$\|\mathbf{x}\|_p := \left( \sum_{i=1}^n |x_i|^p \right)^{1/p} \quad (3.3)$$

$$z_i \rightarrow \frac{z_i}{\|z_i\|_p} \quad (3.4)$$

The results of transforming the original constellation points for 8-PSK can be seen in figure 3.1, note that the results for some other constellation sizes  $M$  are also included. As can be seen in the figure 3.1, when using a permutation that is optimal for the infinity norm  $\|\cdot\|_\infty$  the EE remains  $d_{min}^2 = 3$  for at least  $M = 8, 100 \geq p \geq 1$ . This implies that not all of the optimal permutations are equal in nature, since the other cases in the figure only uses a permutation that was optimized for the 2-norm, and not the infinity-norm.

### 3.4 Multiple layers of permutation

To further improve the EE, it could be worthwhile to use chains of permutations. One way to implement this, for every new permutation that is used, a copy of the current constellation points are created and then permuted, and then added to the high-dimensional constellation containing the current points. That way, the total number of constellation points for a symbol alternative  $S_i$  will grow exponentially,

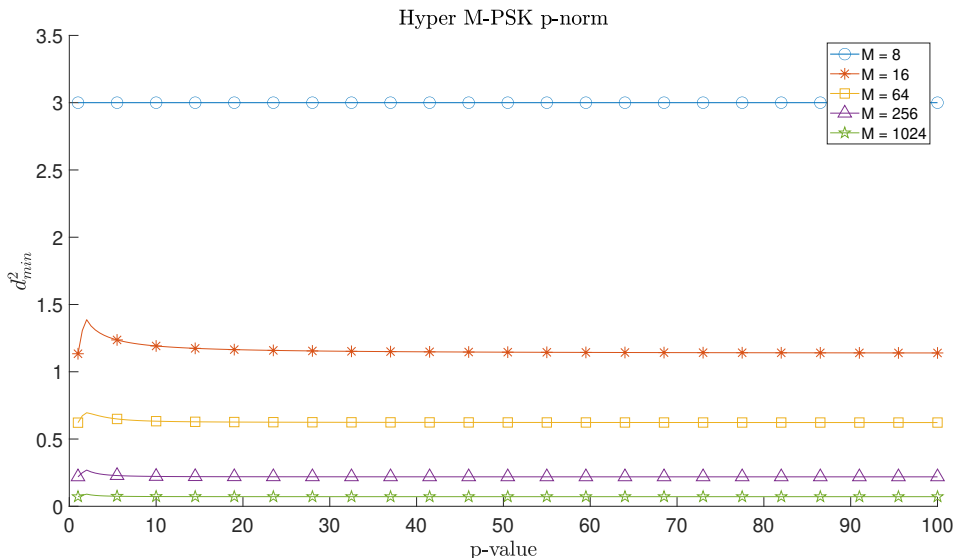


**Figure 3.1:** The EE  $d_{min}^2$  versus the value of  $p$  that is used for the  $p$ -norm for various M-PSK constellations. Only one layer of permutation is used.

$n_{points} = 2^{n_{perm}}$ . Also see table 3.3 for an example of when three permutations are used. An important motivation is that it is expected that if multiple permutations are used, the average energy per bit  $E_b$  for a single permuted constellation will remain unchanged, meaning that the task of improving the EE  $d_{min}^2$  is equivalent to maximizing the minimum Euclidean distance  $D_{min}$  for a constellation. This way, strategies where constellation points are removed in order to improve  $E_b$  can be avoided. Note that when one or several permutations are used, the  $E_b$  for the entire set of constellations will inexorably increase as the number of symbol energies increases, since the number of symbol alternatives  $M$  remains unchanged. This leads to a new definition of the optimization problem, see equation (3.5), while equation (3.2) for the EE remains unchanged. Another important motivation for chained permutations is that the search span does not grow in a factorial manner, which simplifies the search for good permutations and the optimal one.

$$E_b = \frac{1}{k} \times \frac{1}{M} \times \frac{1}{R} \times 2^{n_{perm}} \sum_{i=0}^{M-1} E_i, E_i = |z_i|^2 \quad (3.5)$$

As a direct consequence of using multiple permutations, the effective bit rate  $R_b$  decreases exponentially,  $R_{b,eff} = \frac{1}{2^{n_{perm}}} R_b$ , furthermore the spectral efficiency  $\rho$  also decreases exponentially, see equation (3.6) [10, Eq. (2.21)], where  $W$  [Hz] is the total bandwidth used. The relation between spectral efficiency and EE can be seen in section 3.9. Under ideal conditions,  $\rho_{BPSK} = 1$ , resulting in equation (3.7).

$$\rho = \frac{R_b}{W} \rightarrow \rho = \frac{1}{2^{n_{perm}}} \frac{R_b}{W} [\text{bps}/\text{Hz}] \quad (3.6)$$

$$\rho = \frac{1}{2^{n_{perm}}} \log_2(M) [\text{bps}/\text{Hz}] \quad (3.7)$$

High-dimensional constellation

$P_0$   
 $P_1P_0$   
 $P_2P_0$   
 $P_2P_1P_0$   
 $P_3P_0$   
 $P_3P_1P_0$   
 $P_3P_2P_0$   
 $P_3P_2P_1P_0$

**Table 3.3:** Structure of a high-dimensional constellation when using multiple repetitions with permutations, up to three (3) permutations.  $P_0$  represents the constellation points of the original constellation, whereas  $P_1, P_2, P_3$  represents permutation matrices  $P_i, M \times M$ . Each row represents a permutation of the original constellation points, and each column represents the symbols that has to be sent for a symbol alternative  $S_i$ .

One way of searching for decent permutations when using multiple permutations is to use a heuristic method such as greedy search. The main strategy for greedy algorithms is to choose which option appears to be the most optimal option at the moment [5], which is in this case a permutation for the current permutation layer.

For the purpose of finding decent permutations, a greedy algorithm is implemented the following way in Algorithm 2:

---

**Algorithm 2:** Greedy Search for Decent Permutations

---

**Input:** Number of random permutations  $N_{rand}$ , constellation size  $M$ , constellation points  $\mathbf{z}_1, \mathbf{z}_2, \dots, \mathbf{z}_M$ , number of layers  $L$

**Output:** Best set of permutations, corresponding EE  $d_{min}^2$

- 1 Randomly generate  $N_{rand}$  permutations  $\sigma$ ;
  - 2 Put the permutations  $\sigma$  in list  $\mathcal{L}$ ;
  - 3 Evaluate list  $\mathcal{L}$  using Algorithm 1;
  - 4 Select the best permutations and store them in Layer 1 list  $\mathcal{L}_1$ ;
  - 5 **foreach** permutation  $\sigma_1 \in \mathcal{L}_1$  **do**
  - 6     Initialize chosen permutation set  $\mathcal{S} \leftarrow \{\sigma_1\}$ ;
  - 7     **for**  $\ell = 2$  **to**  $L$  **do**
  - 8         Generate candidate permutations for layer  $\ell$  using remaining eligible permutations from  $\mathcal{L}$ ;
  - 9         For each candidate, form a high-dimensional constellation combining  $\mathcal{S}$  and the candidate permutation;
  - 10         Evaluate all candidates using Algorithm 1;
  - 11         Select the best permutation  $\sigma_\ell$  for current layer and add to  $\mathcal{S}$ ;
  - 12         Return non-chosen permutations to eligible pool  $\mathcal{L}$  for next layer;
  - 13 Display EE  $d_{min}^2$  for best set of permutations found;
  - 14 Display best set of permutations found;
- 

### 3.5 Multiple layers of encoding

In the ideal case the permutation scheme works in conjunction with other previously established bit coding schemes, such as block codes and random interleaving, in order to further lower the BER. In the case of using a block code such as Hamming(7,4), the coding scheme takes four bits and return a codeword of seven bits, enabling it to correct single bit errors and detect double bit errors [8]. This way the EE would first be improved by the block code, and then further improved by the permutation scheme. When using the block code Hamming(7,4), the EE can be written as in equation (3.8) since the minimum distance between codewords is  $D_H = 3$ , and more energy per information bit is required due to the coding rate  $r_c = 4/7$ . This infers that the energy efficiency should be about 71% larger than before, and be compatible with the permutation scheme. For the union bound calculations only the theoretical result of using the Hamming(7,4) code is considered, with no actual simulation being done.

$$d_{min}^2 = \frac{D_H D_{min}^2}{2E_b \frac{1}{r_c}} = \frac{3 \times D_{min}^2}{2E_b \frac{7}{4}} \approx 1.71 \frac{D_{min}^2}{2E_b} \quad (3.8)$$

In the case of also using random interleaving in conjunction with the other schemes, it would not improve the energy efficiency directly, instead it would simply help guarding the transmitted signal against bursty noise [1]. For other bit-level coding strategies interleaving further enables more efficient decoding.

## 3.6 Overview of collected data for M-PAM, M-PSK and M-QAM permutations

In the tables of collected data, the theoretical results for also using the Hamming(7,4) code is included in order to analyze the effects of using multiple error correcting codes. In the case of 8-PAM and 8-PSK when using a single permutation, exhaustive search was conducted while using Algorithm 1. In the case of when  $M > 8$ , and a single permutation was used, the search was conducted using the conjectures outlined in the background section. Finally, for all other cases Algorithm 2 was used.

For M-PAM the best results so far can be seen in table 3.4. These results infer that as the number of permutations increases, the EE will also increase. Some of the permutations are included in appendix A.

For M-PSK the foremost results yet can be seen in table 3.5. Like in the case with M-PAM, the EE increases as the number of permutations increases. Some of the permutations are included in appendix A.

For M-QAM the foremost results so far can be seen in table 3.6, which once again displays the trend that the EE increases as the number of permutations increases. Some of the permutations are included in appendix A.

As a summation of the results so far, it can be inferred that as one or multiple permutations are used, the EE inexorably increases as predicted. Note that in the cases where  $M > 8$  the permutations were found using a heuristic method, meaning there are no guarantees that these are the optimal permutations unlike in the first section 3.1 where exhaustive search was used.

## 3.7 Trend analysis and implications for using multiple layers of permutation

### 3.7.1 Distribution of minimum distances for 16-PAM and 16-QAM

The distribution of minimum distances  $d_{i,min}^2$  for 16-PAM and 16-QAM can be seen in figures 3.2 and 3.3 respectively, in both cases a single permutation is used. From these figures it can be conjectured that at least in the case when one permutation is used, if every minimum distance  $d_{i,min}$  is equal to the lowest minimum distance in the constellation,  $d_{min,lowest}$  then that particular permutation can be considered to be optimal.

$d_{min}^2$	$d_{min, H(7,4)}^2$	$M$	$n_{permutations}$
0.8	1.368	4	0
0.286	0.489	8	0
1.143	1.959	8	1
2.429	4.163	8	2
3	5.143	8	3
3	5.143	8	4
3.143	5.388	8	5
0.094	0.161	16	0
0.8	1.371	16	1
1.577	2.703	16	2
2.012	3.449	16	3
3.035	5.203	16	4
3.371	5.778	16	5
0.009	0.015	64	0
0.2857	0.490	64	1
0.3582	0.614	64	2
1.247	2.138	64	3
2.455	4.208	64	4
3.343	5.730	64	5
0.0007	0.001	256	0
0.0941	0.161	256	1
0.1529	0.262	256	2
0.7119	1.220	256	3
1.8973	3.253	256	4
3.3004	5.658	256	5

**Table 3.4:** The EE values for M-PAM, also includes the cases where the block code Hamming(7,4) is used, labeled as H(7,4).

$d_{min}^2$	$d_{min, H(7,4)}^2$	$M$	$n_{permutations}$
2	3.42	4	0
0.879	1.503	8	0
3	5.143	8	1
3	5.143	8	2
3	5.143	8	3
3	5.143	8	4
3.1875	5.464	8	5
0.304	0.521	16	0
1.387	2.378	16	1
2.673	4.583	16	2
3.159	5.416	16	3
3.639	6.238	16	4
3.888	6.665	16	5
0.029	0.049	64	0
0.6954	1.192	64	1
1.2254	2.102	64	2
2.642	4.529	64	3
3.5356	6.061	64	4
4.3633	7.480	64	5
0.002	0.004	256	0
0.2692	0.461	256	1
0.4391	0.753	256	2
1.7747	3.042	256	3
3.3832	5.800	256	4
4.7715	8.180	256	5

**Table 3.5:** The EE values for M-PSK, also includes the cases where the block code Hamming(7,4) is used, labeled as H(7,4).

$d_{min}^2$	$d_{min, H(7,4)}^2$	$M$	$n_{permutations}$
2	3.42	4	0
0.8	1.368	16	0
2	3.429	16	1
2.2	3.771	16	2
2.9	4.971	16	3
3.4	5.829	16	4
3.725	6.386	16	5
0.286	0.489	64	0
1.143	1.959	64	1
1.429	2.449	64	2
2.429	4.163	64	3
3.464	5.939	64	4
4.188	7.179	64	5
0.094	0.161	256	0
0.471	0.807	256	1
0.706	1.210	256	2
1.977	3.388	256	3
3.288	5.637	256	4
4.485	7.689	256	5

**Table 3.6:** The EE values for M-QAM, also includes the cases where the block code Hamming(7,4) is used, labeled as H(7,4).

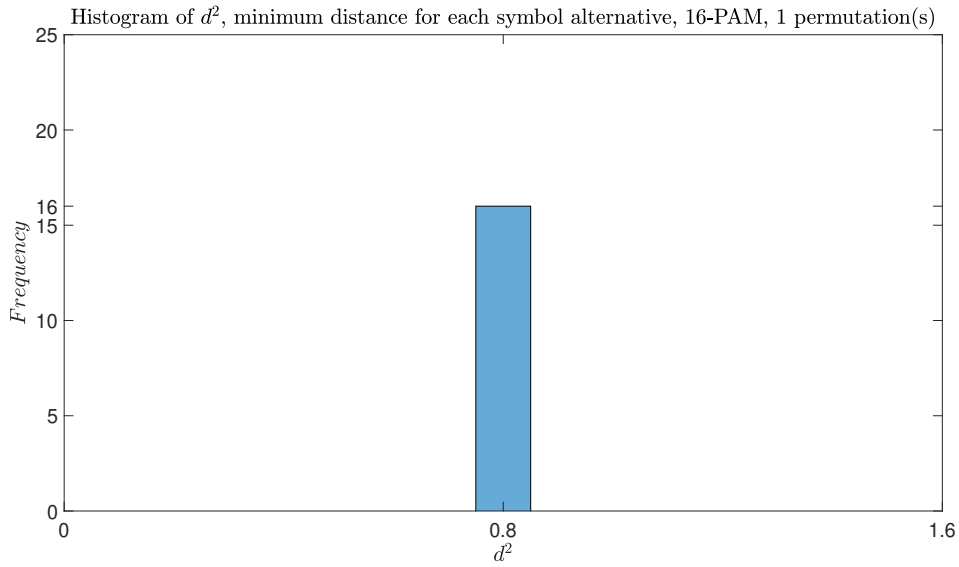


**Figure 3.2:** Histogram for the minimum distances in a 16-PAM constellation where one (1) permutation is used.

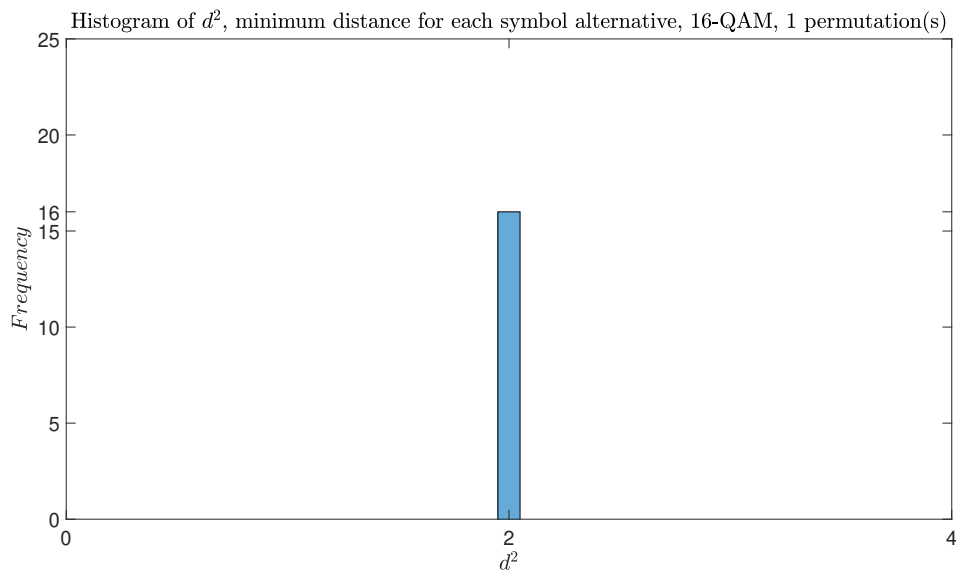


**Figure 3.3:** Histogram for the minimum distances in a 16-QAM constellation where one (1) permutation is used.

### 3.7.2 Union bounds for 16-PAM and 16-QAM

Figures 3.4, 3.5 display the union bounds, or the upper bounds for the symbol error probability  $P_s$  for the 16-PAM- and 16-QAM constellations respectively, where one(1) permutation is used in both cases. What stands out in these two figures is that the union bounds are still mostly determined by the lowest normalized minimum distance  $d_{min}^2$  in the respective constellations.

### 3.7.3 Distribution of all distances for 256-QAM constellations

In the figures 3.6, 3.7 and 3.8 the distribution of all normalized squared Euclidean distances  $d^2$  for the 256-QAM constellations that uses one, three and five permutations respectively can be seen. These figures indicate that when using permutations the distances in at least 256-QAM constellations resembles a Rayleigh distribution [3]. It can also be seen that when more permutation layers are used, increasing the total number of distances, the histogram for all distances starts to resemble a normal distribution instead, which can be explained by the central limit theorem [3].

### 3.7.4 256-QAM union bounds

Figures 3.9, 3.10, 3.11 show the union bounds, or the upper bounds for the symbol error probability  $P_s$  for 256-QAM constellations that use one, three and five permutations respectively. What can be clearly seen in figure 3.10 by comparing the hyper 256-QAM uncoded curve to the binary signaling one is that the value of the union bound is no longer only determined by the lowest minimum

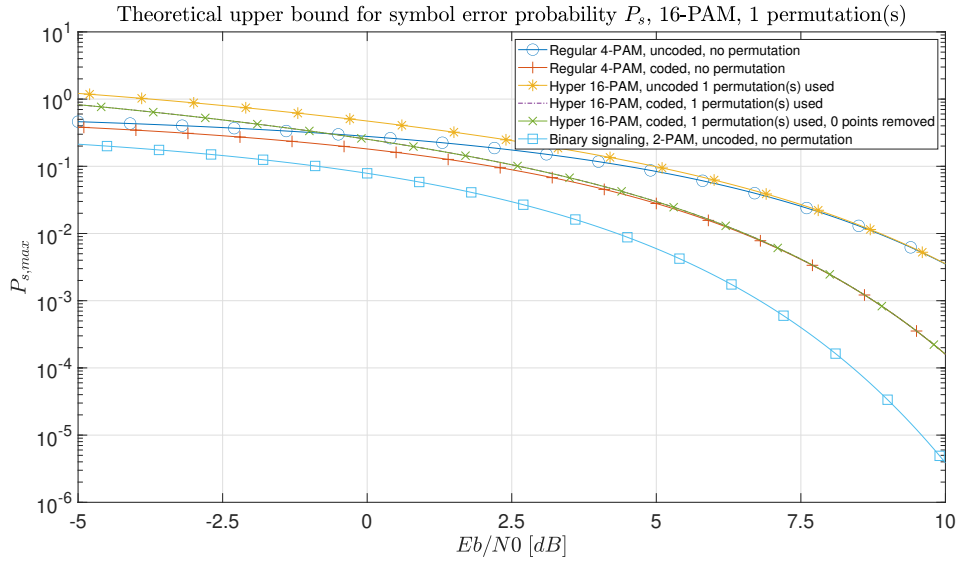


**Figure 3.4:** Plot of the union bound for 16-PAM, where one (1) permutation is used. Regular 4-PAM and uncoded binary signaling (BPSK) are used for comparison.

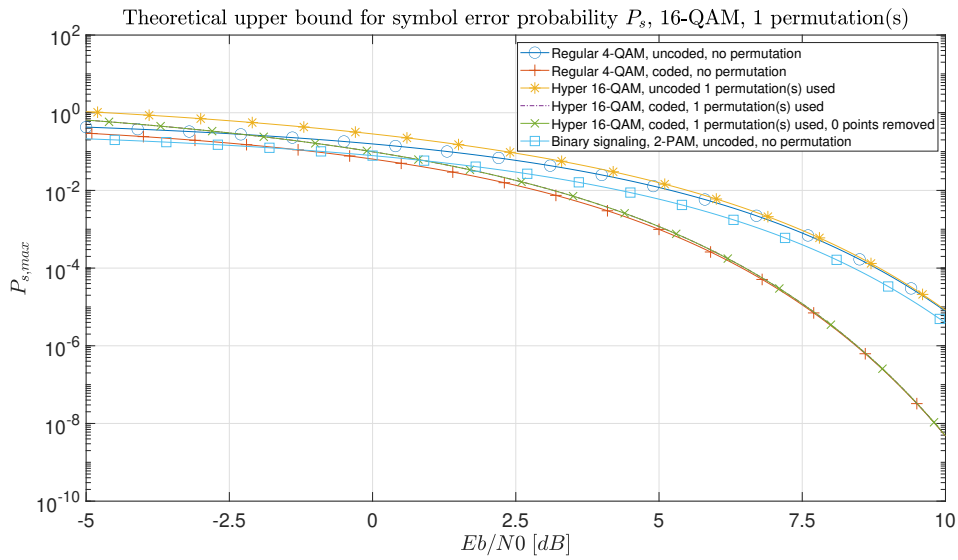


**Figure 3.5:** Plot of the union bound for 16-QAM, where one (1) permutation is used. Regular 4-QAM and uncoded binary signaling (BPSK) are used for comparison.

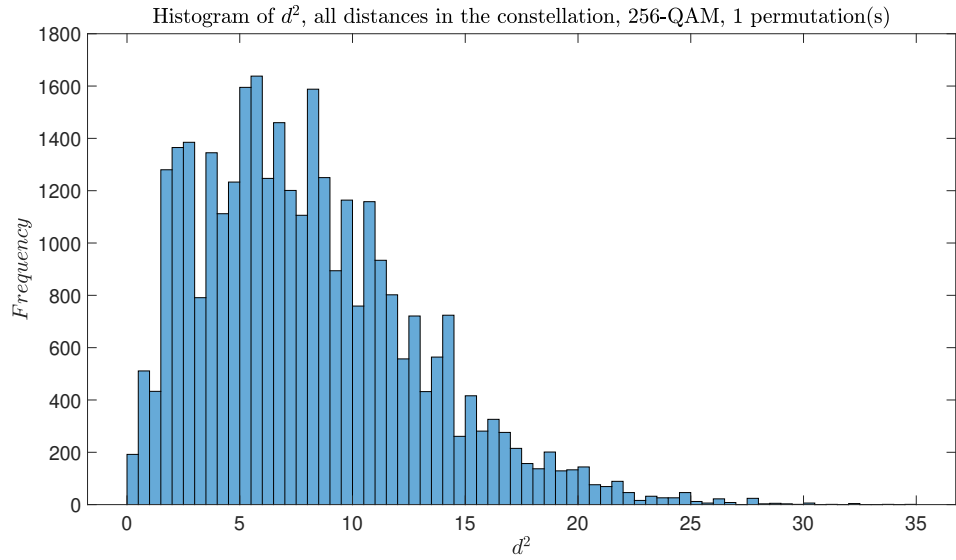


**Figure 3.6:** Distribution of all distances in a 256-QAM constellation where one (1) permutation is used.

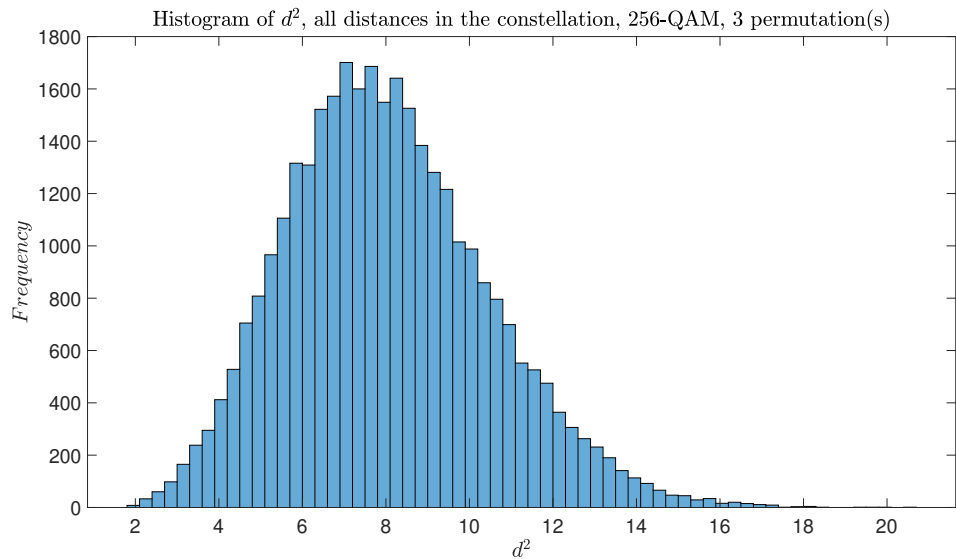


**Figure 3.7:** Distribution of all distances in a 256-QAM constellation where three (3) permutations are used.

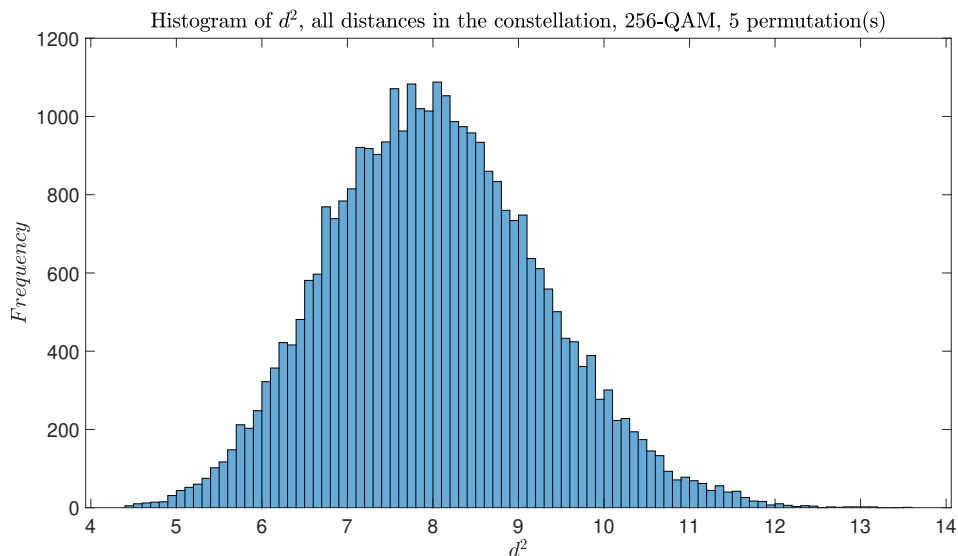


**Figure 3.8:** Distribution of all distances in a 256-QAM constellation where five (5) permutations are used.

distance  $d_{min}^2$ , but also by the number of occurrences  $c_1$  for the lowest minimum distance in the constellation. In both figures 3.10, 3.11 what stands out is that when constellation points are strategically removed, the union bounds are lowered even further after using multiple permutation. This is because as the smallest distances from the constellation are removed, the value of the union bound has to theoretically decrease.

### 3.8 Wireless channel simulation

To test the permutation scheme a simple simulation is used where the wireless channel only considers complex AWGN. For AWGN the mean and the variance values respectively of the noise are modeled with equation (3.9), [10, Eq. (5.22)], assuming the received noisy vector  $\mathbf{r}$  has  $N$  dimensions. Since AWGN is additive, the relation between the received noisy vector  $\mathbf{r}$  and the transmitted signal vector  $\mathbf{z}_j$  (for symbol alternative  $S_j$ ) is given by equation (3.10), [10, Eq.(5.18)].

$$\begin{aligned}
 m &= E\{w_l\} = 0 \\
 \sigma_l^2 &= E\{w_l^2\} = \frac{N_0}{2}, \quad -\infty \leq f \leq \infty \\
 E\{w_l w_m\} &= 0, \quad l \neq m, \quad l = 1, 2, \dots, N
 \end{aligned} \tag{3.9}$$

$$\mathbf{r} = \mathbf{z}_j + \mathbf{w} \tag{3.10}$$

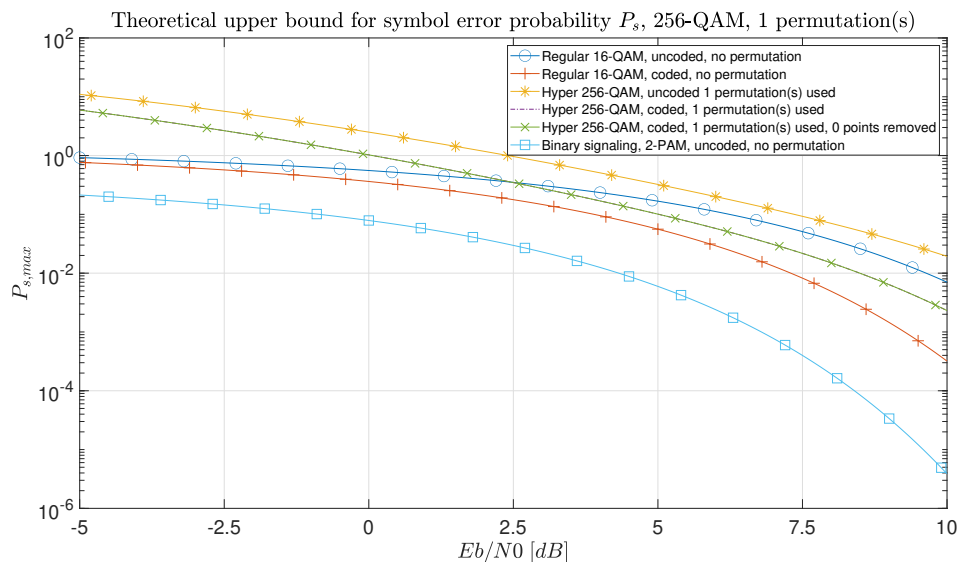


**Figure 3.9:** Union bound, or the upper symbol error probability bound for 256-QAM where one (1) permutation is used. Regular 16-QAM and uncoded binary signaling (BPSK) are used for comparison.

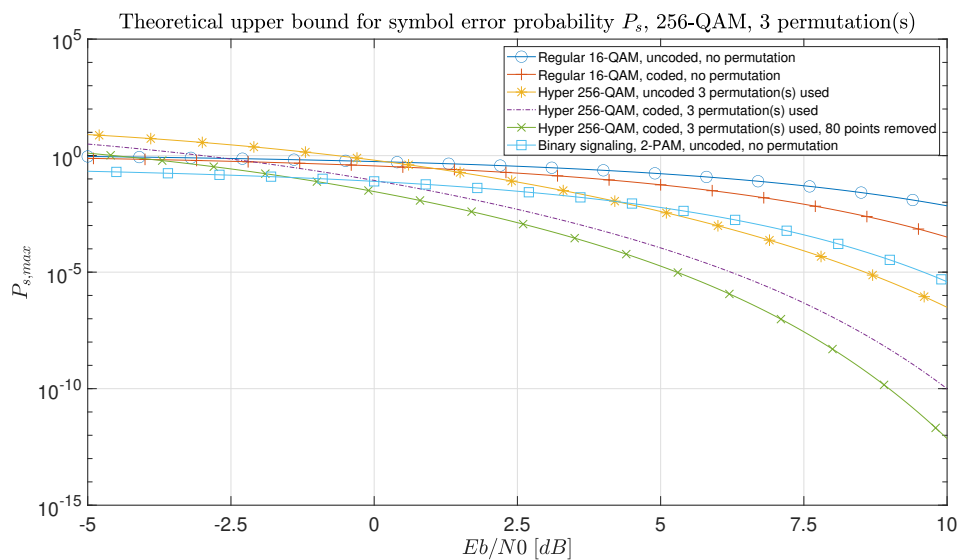


**Figure 3.10:** Union bound, or the upper symbol error probability bound for 256-QAM where three (3) permutations are used. Regular 16-QAM and uncoded binary signaling (BPSK) are used for comparison.

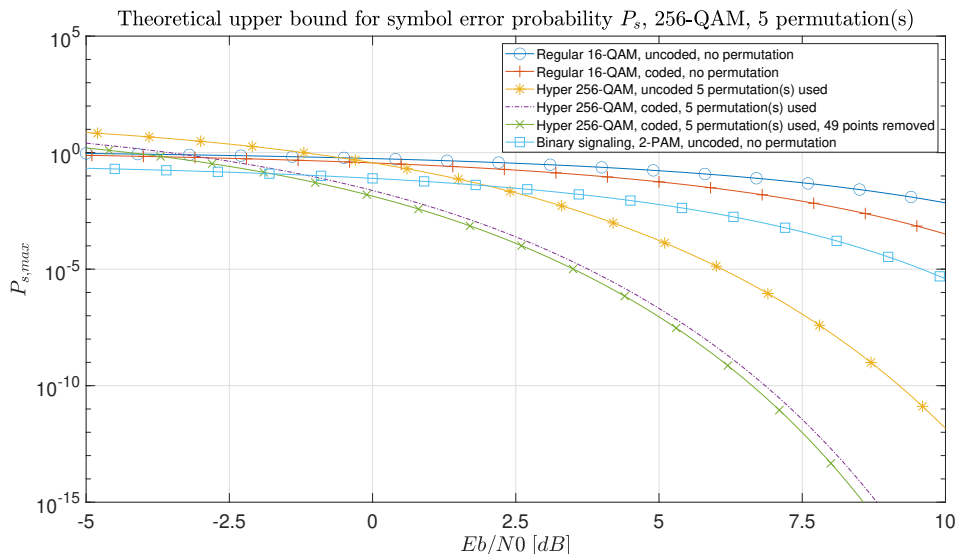


**Figure 3.11:** Union bound, or the upper symbol error probability bound for 256-QAM where five (5) permutations are used. Regular 16-QAM and uncoded binary signaling (BPSK) are used for comparison.

The simulated transmitter uses random interleaving (to test for compatibility) for all constellations, while there is both a coded and a non-coded transmission for each constellation, with the exception of the (BPSK) constellation which does not use a block code. The binary code that is used in the transmitter is the block code Hamming(7,4), which subsequently gives a coding rate of  $R_c = \frac{4}{7}$  when used. In the simulation the Hamming(7,4) code is used to encode all of the information bits by adding redundant parity bits, so that single bit errors may be corrected at the receiver. Both the transmitter and receiver use gray bit mapping, meaning that adjacent symbol alternatives  $S_i$  in a constellation will only differ in one bit.

The simulated receiver is based on the Maximum-Likelihood (ML) receiver which assumes that all message alternatives are equally likely, resulting in the decision rule (3.11), [10, Eq. (5.28)]. The message alternative that is chosen is determined by which option produces the smallest squared Euclidean distance with the received vector. The BER for each separate transmission is calculated using equation (3.12).

$$\hat{m}(r) = m_l \Leftrightarrow \min_{\{i\}} D_{r,i}^2 = D_{r,l}^2 \quad (3.11)$$

$$BER = \frac{\text{number of incorrectly received info. bits}}{\text{total number of received info. bits}} \quad (3.12)$$

In the figures 3.12, 3.13 the BER for the constellation 8-PSK is displayed for one and three permutations respectively. As expected they have similar BER

curves, since they have identical EE  $d_{min}^2 = 3$ . While using 8-PSK with multiple permutations does result in a more favorable distribution of minimum distances  $d^2$ , the BER is still overwhelmingly determined by the value of the EE.

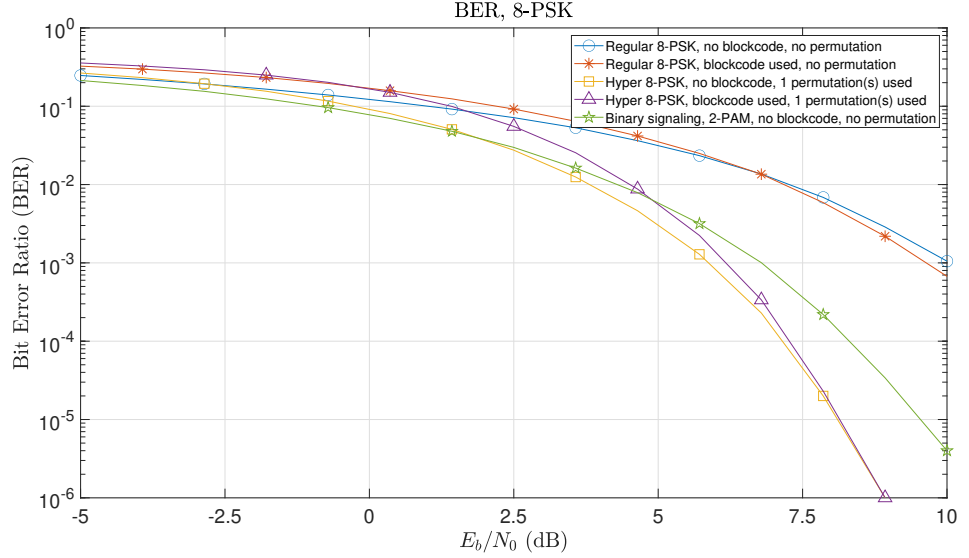


**Figure 3.12:** Plot of the BER for 8-PSK where one (1) permutation is used. Regular 8-PSK and uncoded binary signaling (BPSK) is used for comparison. The number of transmitted information bits is 1 000 000.

In figures 3.14, 3.15 and 3.16 the BER for the constellation 256-QAM is displayed for one, three and five permutations respectively. Like in the case of 8-PSK, it can clearly be seen that the BER is mostly determined by the EE. It can also be seen that there is a minimum  $\frac{E_b}{N_0}$  before the curves that uses the blockcode Hamming(7,4) overtakes the curves that does not. This behaviour can be explained by the fact that as several error correcting codes are used the total coding rate  $R$  grows in value, meaning that the average energy per bit  $E_b$  also grows in value. For a fixed ratio  $E_b/N_0$ ,  $N_0$  will have to be larger to compensate for the lower coding rate  $R$ , and since Hamming(7,4) can only correct one bit error per codeword, it is not enough to compensate the larger  $N_0$  at lower  $E_b/N_0$ .

### 3.9 Energy Efficiency and Spectral Efficiency Comparison

The graph 3.17 compares the ideal spectral efficiency  $\rho$  for uncoded 256-QAM with its EE. The spectral efficiency  $\rho$  is calculated using equation (3.7). What stands out in the figure is how much the EE can be improved before spectral efficiency is lowered too much, meaning that it also shows how many permutations can reasonably be used for actual transmissions.

The tables 3.7, 3.8 and 3.9 show the spectral efficiency  $\rho$  and  $E_b/N_0$  for various constellations under the condition that the symbol error probability  $P_s$  is  $P_s =$

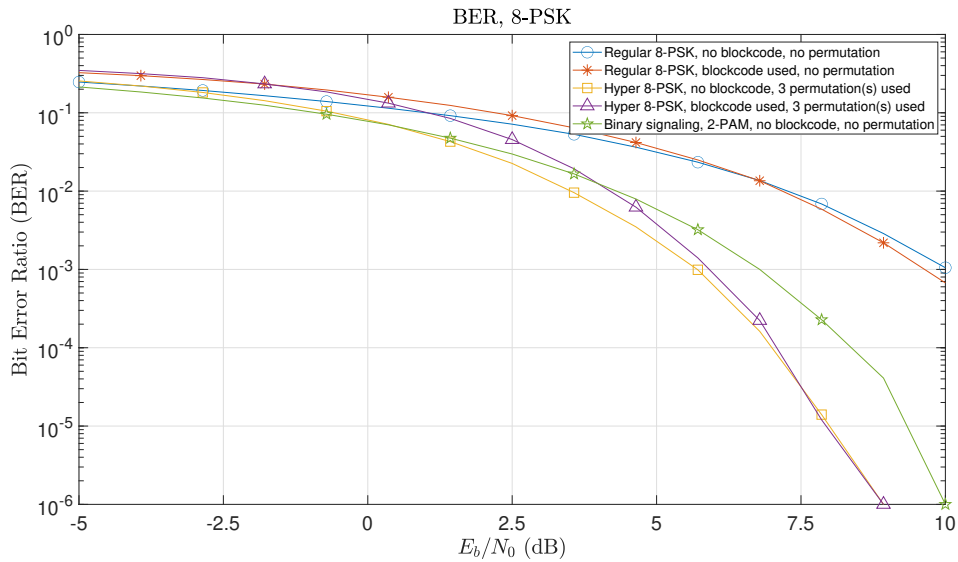


**Figure 3.13:** Plot of the BER for 8-PSK where three (3) permutations are used. Regular 8-PSK and uncoded binary signaling (BPSK) is used for comparison. The number of transmitted information bits is 1 000 000.

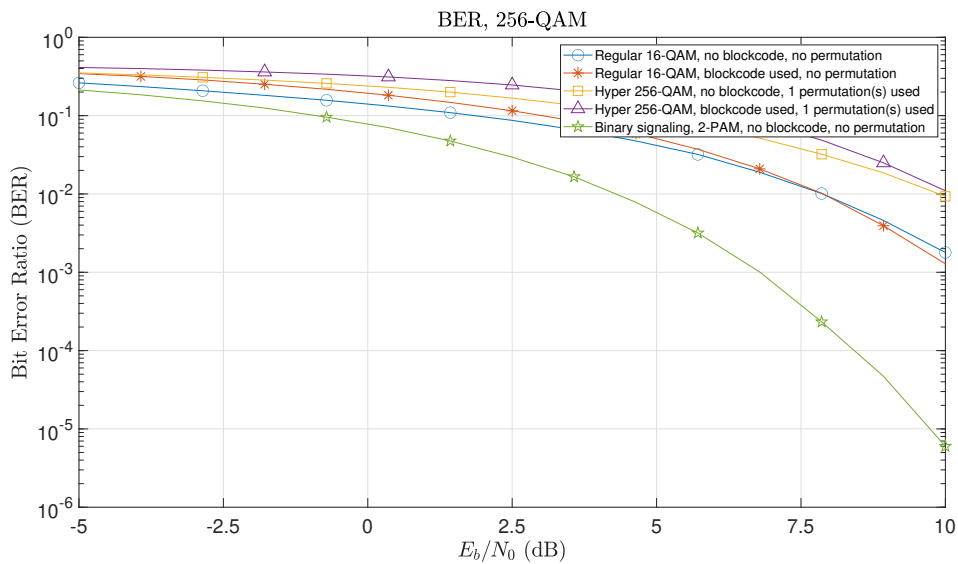


**Figure 3.14:** Plot of the bit error ratio for 256-QAM where one (1) permutation is used. Regular 16-QAM and uncoded binary signaling (BPSK) is used for comparison. The number of transmitted information bits is 1 000 000.

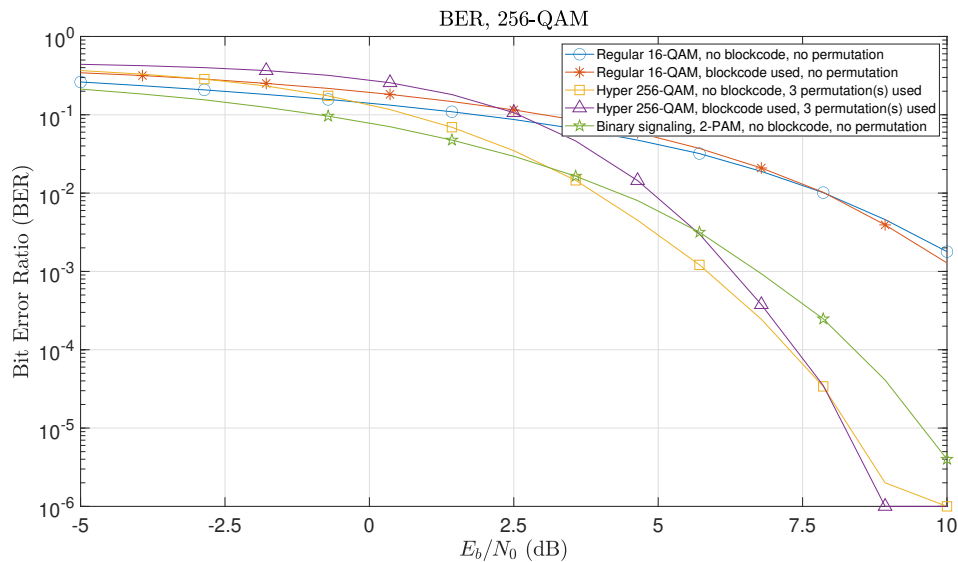


**Figure 3.15:** Plot of the BER for 256-QAM where three (3) permutations are used. Regular 16-QAM and uncoded binary signaling (BPSK) is used for comparison. The number of transmitted information bits is 1 000 000.

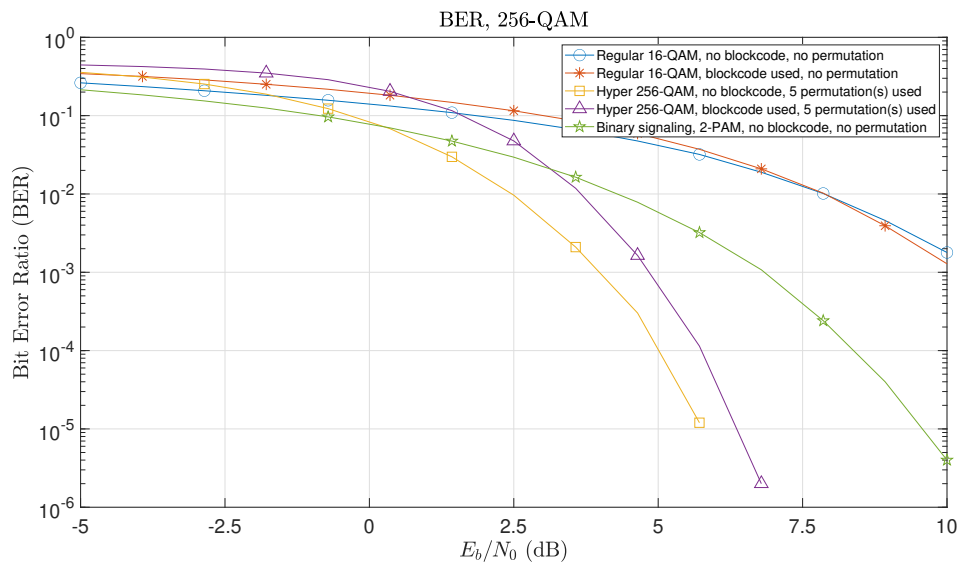


**Figure 3.16:** Plot of the BER for 256-QAM where five (5) permutations is used. Regular 16-QAM and uncoded binary signaling (BPSK) keying is used for comparison. The number of transmitted information bits is 1 000 000.

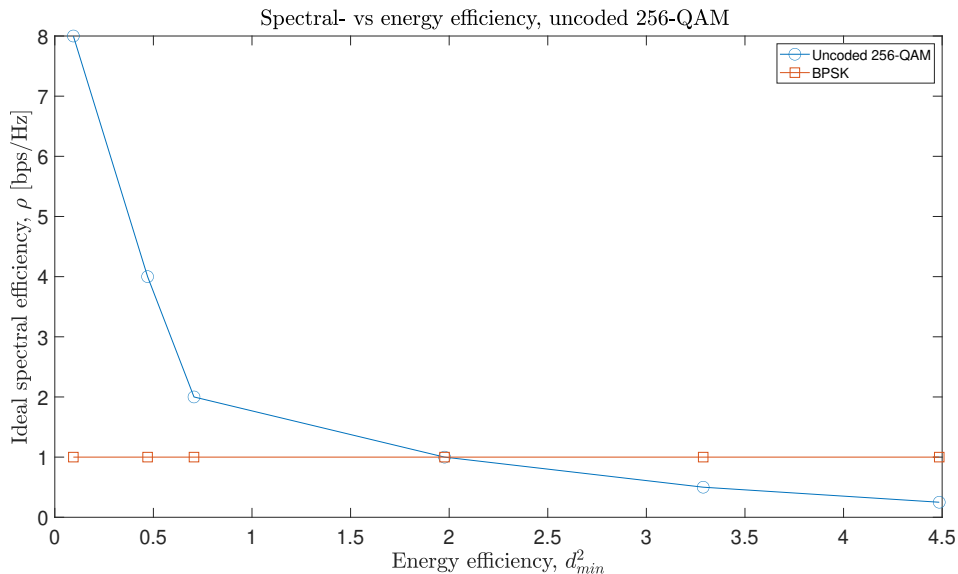


**Figure 3.17:** Plot of the ideal spectral efficiency compared to the EE of uncoded 256-QAM, the spectral efficiency is calculated for the effective bit rate. Uncoded BPSK is used for comparison.

$10^{-5}$ . The spectral efficiencies were calculated using equation (3.7), while the values for  $E_b/N_0$  were obtained by plotting the union bound using equation (2.17), and then observing the value of  $E_b/N_0$  for  $P_s = 10^{-5}$ . As indicated earlier in the chapter, the tables show that as the EE  $d_{min}^2$  increases,  $E_b/N_0$  is smaller for the same symbol error probability  $P_s$ . The figure 3.18 show the proximity of the spectral efficiencies to the capacity curve  $C/W$  given by Shannon's channel capacity theorem. One notable trend is that when three (3) layers of permutations are used, the different constellations seem to converge to a particular point.

$\rho$ (bps/Hz)	$E_b/N_0$ (dB)	M	$n_{perm}$	$\rho$ (bps/Hz)	$E_b/N_0$ (dB)	M	$n_{perm}$
3	18.3	8	0	3	13.5	8	0
1.5	11.8	8	1	1.5	8.3	8	1
0.4	8.3	8	3	0.4	8.1	8	3
4	23.1	16	0	4	18.1	16	0
2	13.8	16	1	2	11.2	16	1
0.5	9.0	16	3	0.5	7.7	16	3

**Table 3.7:** Spectral efficiency  $\rho$  and SNR  $E_b/N_0$  for  $M$ -PAM. The symbol error probability is  $P_s = 10^{-5}$ .

**Table 3.8:** Spectral efficiency  $\rho$  and SNR  $E_b/N_0$  for  $M$ -PSK. The symbol error probability is  $P_s = 10^{-5}$ .

$\rho$ (bps/Hz)	$E_b/N_0$ (dB)	M	$n_{perm}$
4	14.0	16	0
2	9.9	16	1
0.5	8.0	16	3
8	23.4	256	0
4	15.8	256	1
1	8.6	256	3
0.25	6.1	256	5

**Table 3.9:** Spectral efficiency  $\rho$  and SNR  $E_b/N_0$  for  $M$ -QAM. The symbol error probability is  $P_s = 10^{-5}$ .

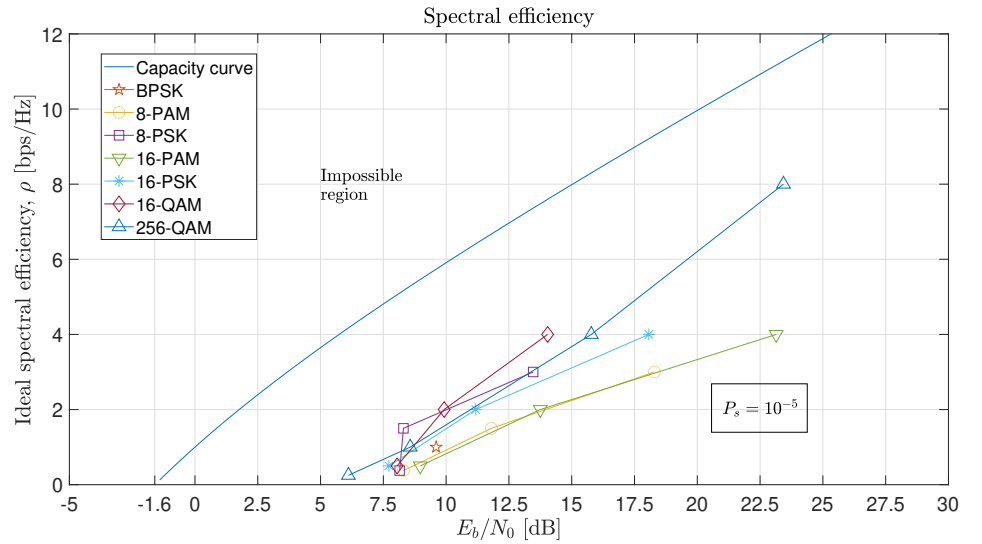


**Figure 3.18:** Plot of ideal spectral efficiencies vs. the minimum values of  $E_b/N_0$  needed to achieve the symbol error probability  $P_s = 10^{-5}$ , for various constellations. See tables 3.7, 3.8 and 3.9 for the corresponding number of permutations. The capacity curve is given by  $C/W$ , which is derived from Shannon's theorem on channel capacity.

## 4.1 Summary and conclusions

To summarize, the goal of this project was to develop a new permutation-based repetition coding-like error correcting code that is as energy efficient as possible. To this end, both exhaustive search and randomized search of permutations was conducted, with a greedy search algorithm being used for the case when multiple permutations are used. It was inferred that as permutations are used the EE does increase, with an improved simulated BER as a direct result. As a direct consequence of using permutations, the effective bit rate and thus the spectral efficiency decreases exponentially with the number of permutations.

As a conclusion, not only do these optimal permutations exist for the three types of investigated modulation schemes and do indeed increase the EE, but the optimal EE for 8-PAM and 8-PSK has been determined via exhaustive search. The potential to increase the EE for various constellations underlines how much more energy efficient and reliable devices could be.

The patterns for optimal permutations in the first layer seems to be all cyclical in nature. This seem plausible since ordering the constellation points in a cyclical way then makes sure that previously adjacent symbol alternatives are no longer adjacent, but rather as far away from each other as possible, maximizing the minimum Euclidean distance for the constellation.

The local search method derived for this thesis was the greedy search algorithm, which enabled finding sets of multiple permutations from a limited set of randomly generated permutations. While the upper bounds for the EE are yet to be determined, the lower bounds can be defined as the best results found so far.

In the case of how the optimal permutations for 8-PSK were affected when normalizing constellation points with their respective p-norms, it was found that the EE can not be improved this way. However it was also found that only the permutations which were optimal for the infinity norm, remained optimal for all values of p. This implies that at least for optimal M-PSK permutations there is some innate quality which sets them apart.

It was found that in general when using multiple permutations the EE experiences a significant increase beyond the results of using one singular permutation, and that the value of the union bound is lowered as a direct consequence. It was also found that the distribution of the Euclidean distances in a constellation changes in such a way that it could also contribute to decreasing the BER. While the distribution of distances in a constellation is at first sight seemingly Rayleigh distributed, at least for 256-QAM it then starts to resemble as normal distribution as the total number of permutation layers, and thus distances increases.

In the simulations it could be seen that the permutation scheme does work in conjunction with previously established binary coding schemes, such as random interleaving and block codes, and that binary coding scheme used with binary antipodal signaling can be surpassed.

## 4.2 Future work

The most pressing unanswered questions is how to determine whether a permutation is optimal or not, and how to find optimal permutations when multiple permutations are used. One other thing to be investigated is how well the permutation scheme works in an actual transmission.

To determine whether a permutation is optimal or not it is conjectured that if all minimum distances between constellation points in a constellation are equal to the lowest possible minimum distance, then that permutation can be considered to be optimal, though at this time there is no formal proof for that statement.

In the case of using multiple permutations, the search space for permutations could in theory be reduced by applying some preliminary conditions to what the structure of permutations is allowed to be. One such condition could be that previously adjacent symbol alternatives are not allowed to be adjacent in the permutation, at least in the first layer. When using multiple permutations the structure of each permutation chosen by the greedy search method is not as obvious as in the case of using one permutation, meaning that in order to find a better local search method than greedy search the structures of the permutations would first have to be carefully examined.

---

## References

---

- [1] K. Andrews, C. Heegard, D. Kozen, *A Theory of Interleavers.*, Tech. Rep. TR97-1634, Computer Science Department, Cornell University, Jun. 1997.
- [2] E. Arikan, *Channel polarization: A method for constructing capacity-achieving codes*, 2008 IEEE International Symposium on Information Theory, Toronto, ON, Canada, 2008, pp. 1173-1177, doi: 10.1109/ISIT.2008.4595172.
- [3] G. Blom, J. Enger, G. Englund, J. Grandell, and L. Holst, *Sannolikhetsteori och statistikteori med tillämpningar*. 7th ed. Lund: Studentlitteratur AB, 2017.
- [4] C. Berrou, A. Glavieux and P. Thitimajshima, *Near Shannon limit error-correcting coding and decoding: Turbo-codes. 1*, Proceedings of ICC '93 - IEEE International Conference on Communications, Geneva, Switzerland, 1993, pp. 1064-1070 vol.2, doi: 10.1109/ICC.1993.397441.
- [5] P.E. Black, *"greedy algorithm"*, in *Dictionary of Algorithms and Data Structures [online]*, Paul E. Black, ed. 2 February 2005. (accessed 2025-04-22) Available from: , <https://www.nist.gov/dads/HTML/greedyalgo.html>
- [6] P. Elias, *Error-free Coding*, in Transactions of the IRE Professional Group on Information Theory, vol. 4, no. 4, pp. 29-37, September 1954, doi: 10.1109/TIT.1954.1057464.
- [7] R. Gallager, *Low-density parity-check codes*, in IRE Transactions on Information Theory, vol. 8, no. 1, pp. 21-28, January 1962, doi: 10.1109/TIT.1962.1057683.
- [8] R. W. Hamming, *Error detecting and error correcting codes*, in The Bell System Technical Journal, vol. 29, no. 2, pp. 147-160, April 1950, doi: 10.1002/j.1538-7305.1950.tb00463.x.
- [9] K. Ivanov, W. Yang, and J. Jiang, *Probabilistic Shaping in MIMO: Going Beyond 1.53dB AWGN Gain With the Non-Linear Demapper*, arXiv preprint arXiv:2504.18459, 2025. Available at: <https://arxiv.org/abs/2504.18459>
- [10] G. Lindell, *Introduction to Digital Communications*. Lund: Lund University, 2013.

- [11] A.F. Molisch, *Wireless Communications*. 2nd ed. Hoboken, NJ: Wiley-IEEE Press, 2011.
- [12] V. Pless, *Introduction to the theory of error-correcting codes*. New York: Wiley, 1982.
- [13] C.E. Shannon (1948), *A Mathematical Theory of Communication*, Bell System Technical Journal, 27: 623-656. <https://doi-org.ludwig.lub.lu.se/10.1002/j.1538-7305.1948.tb00917.x>
- [14] A. Viterbi, *Error bounds for convolutional codes and an asymptotically optimum decoding algorithm*, in IEEE Transactions on Information Theory, vol. 13, no. 2, pp. 260-269, April 1967, doi: 10.1109/TIT.1967.1054010.

## Optimal permutations

---

In this appendix, there are some selected permutations for various constellations.

16-PAM permutations
4 8 12 16 3 7 11 15 2 6 10 14 1 5 9 13
4 8 12 16 3 7 11 15 1 5 9 13 2 6 10 14
4 8 12 16 2 6 10 14 3 7 11 15 1 5 9 13
4 8 12 16 1 5 9 13 2 6 10 14 3 7 11 15
3 7 11 15 4 8 12 16 2 6 10 14 1 5 9 13
3 7 11 15 4 8 12 16 1 5 9 13 2 6 10 14
2 6 10 14 3 7 11 15 4 8 12 16 1 5 9 13
1 5 9 13 2 6 10 14 3 7 11 15 4 8 12 16

**Table A.1:** Optimal permutations for a 16-ary PAM constellation, in terms of the indices for the original constellation points. Only one layer of permutation is used.

16-PSK permutation
1 12 7 2 13 8 3 14 9 4 15 10 5 16 11 6

**Table A.2:** Optimal permutation for a 16-ary PSK constellation, in terms of the indices for the original constellation points. Only one layer of permutation is used.

16-QAM permutation
5 13 6 14 7 15 8 16 1 9 2 10 3 11 4 12

**Table A.3:** Optimal permutation for a 16-ary QAM constellation, in terms of the indices for the original constellation points. Only one layer of permutation is used.



---

## 8-PSK P-norm explanation

---

The explanation for the 8-PSK p-norm conjecture is as follows below. Assume the original constellation is represented by  $S_{org} = [S_1, S_2, S_3, S_4, S_5, S_6, S_7, S_8]$ , where  $S_i$  is a symbol alternative and that  $S_{perm} = [S_2, S_5, S_8, S_3, S_6, S_1, S_4, S_7]$  represents the permuted constellation. For  $M = 8$  the angles for the constellation points are given by equation (2.4), and their normalization is described by equations (3.3) and (3.4) respectively. Since all constellation points in M-PSK have equal symbol energy, equation (2.10) can be rewritten to (B.1).

$$E_b = \frac{2M}{M \log_2(M)} |z_1|^2 = \frac{2}{\log_2(8)} \left( \sqrt{(1-0)^2 + (0-0)^2} \right)^2 = \frac{2}{3} \quad (\text{B.1})$$

For the squared minimum Euclidean distance, it can be seen using equations (3.1) and (3.2) that for  $(S_1, S_2)$ ,  $d_{1,2}^2 = 3$ , and it is assumed that  $d_{min}^2 = d_{1,2}^2$  for all values of  $p$ . When the two corresponding constellation points are normalized using their p-norms, the distance can be calculated using equation (3.1), see equation (B.2).

$$\begin{aligned} D^2 = \|\mathbf{z}_1 - \mathbf{z}_2\|_2^2 &= \left(1 - \operatorname{Re} \frac{1+i}{2^{1/p}}\right)^2 + \left(0 - \operatorname{Im} \frac{1+j}{2^{1/p}}\right)^2 \\ &\quad + \left(\operatorname{Re} \frac{1+j}{2^{1/p}} - (-1)\right)^2 + \left(\operatorname{Im} \frac{1+j}{2^{1/p}} - (0)\right)^2 \\ &= \left(2 + \frac{4}{2^{2/p}}\right) \end{aligned} \quad (\text{B.2})$$

The resulting  $d_{min}^2$  can then be calculated using equation (B.3), where  $E_b$  is represented accordingly after normalizing the constellation points  $(\mathbf{z}_1, \mathbf{z}_2)$ .

$$d_{min}^2 = \frac{2 + \frac{4}{2^{2/p}}}{2 \cdot \frac{1}{\log_2(8)} \left(1 + \frac{2}{2^{2/p}}\right)} = \log_2(8) = 3 \quad (\text{B.3})$$



**LUND**  
UNIVERSITY

Series of Master's theses  
Department of Electrical and Information Technology  
LU/LTH-EIT 2025-1084  
<http://www.eit.lth.se>